light scattering (DLS) measurements were carried out at 24.5 °C with a DLS-700 instrument (Otsuka Electronics Co., Ltd., Tokyo Japan). Measurement of zeta-potential was performed with an ELSZ-2 instrument (Otsuka Electronics Co., Ltd., Tokyo Japan).

2.2. Animals

Five-week-old ddY female mice and CDF_1 female mice were purchased from the Sankyo Labo Service Corporation, Tokyo, Japan. All animal experiments were carried out in accordance with the guidelines of the Guiding Principles for the Care and Use of laboratory Animals of Hoshi University.

2.3. Synthesis of PEG-P(Lys-DOTA)

A synthesis of a chelate moiety-binding block copolymer is shown in Fig. 1. A poly(ethylene glycol)-*b*-poly(L-lysine) block copolymer (PEG-P(Lys)) was prepared through acid hydrolysis of a poly(ethylene glycol)-*b*-poly[ε-(benzyloxycarbonyl)-L-lysine] (PEG-P(Lys(Z)) block copolymer [26]. We synthesized PEG-P(Lys)s from PEG-NH_2 (molecular weight of PEG-NH_2 = 5200). The compositions of PEG-P(Lys)s were determined by means of ^{1}H NMR in D_2O under an acidic condition. A mixture of PEG-P(Lys) (86.0 mg), and 1,4,7,10-tetraazacyclododecane-1,4,7,10-tetraacetic acid mono (*N*-hydroxysuccinimide ester) (DOTA-OSu, 308.0 mg) in 8.6 mL of dry DMF was stirred, and then, dry triethylamine (0.5 mL) was added to this reaction mixture. The reaction mixture was stirred overnight at 50 °C. The resulting mixture was dialyzed, at first, against 0.02 N HCl and, then, against distilled H_2O 5 times. The obtained polymer was dissolved in H_2O (at a polymer concentration higher than 15 mg/mL) again, and dialyzed against H_2O 3 times, and we obtained poly(ethylene glycol)-*b*-poly(L-lysine-DOTA) (PEG-P(Lys-DOTA)) by means of lyophilization (162.8 mg). The composition of PEG-P(Lys-DOTA) was determined by means of ^{1}H NMR in D_2O under an alkali condition (pH > 10). The number of bound DOTA units per polymer chain was calculated from the peak area ratio among CH_2 protons of PEG at 3.73 ppm, 24H protons of DOTA, and 2H protons of lysine in the range of 3.36–2.18 ppm. ^{1}H NMR (ppm, D_2O + NaOD): 4.08 (s, CH of lysine units), 3.73 (s, CH_2 of PEG), 3.39 (s, OCH_3 of terminal PEG), 3.36–2.18 (m, 24H of DOTA and CH_2 of lysine), and 2.18–1.10 (m, 6H of lysine).

2.4. Gadolinium (III) chelation to PEG-P(Lys-DOTA)

$GdCl_3$·$6H_2O$ (35.0 mg, 0.094 mmol) was added to PEG-P(Lys-DOTA) (153.3 mg) in H_2O (15.0 mL), and the pH of the solution was maintained between 6.0–6.5. The reaction mixture was stirred for 3 h at 50 °C, followed by dialysis against distilled H_2O 5 times. PEG-P(Lys-DOTA-Gd) was obtained as a white solid after lyophilization (160.8 mg). The determination of gadolinium ions in the block copolymer was carried out by means of ICP measurements (7.0 wt.%, the number of gadolinium ions per polymer chain was 6.7). The obtained PEG-P(Lys-DOTA-Gd) is indicated as 118-17-17-7 (PEG unit = 118, lysine units = 17, DOTA moieties = 17, number of gadolinium ion = 7).

2.5. Blood concentration of PEG-P(Lys-DOTA-Gd) micelles in mice

Blood samples (10–75 μL) from the tail vein (n = 3) of mice (ddY) (30–33 g) were collected in heparinized capillary glass. Saline (1.5 mL) was added to the blood samples, and the mixture was centrifuged at 4 °C for 4 min at 13,000 rpm. The supernatant of the plasma solution was collected, and the gadolinium ion contents of the block copolymer were measured by means of ICP. The plasma and blood volume were calculated as 0.0488 mL/g body weight for plasma and 0.0778 mL/g body weight for blood, respectively.

2.6. Biodistribution of the contrast agents

Biodistribution of the contrast agents was evaluated in CDF_1 female mice (5 weeks old) (20–22 g) bearing a colon 26 tumor. Colon 26 cells (1.0×10^4 cells/0.1 mL) were transplanted into CDF_1 female mice subcutaneously. Injection of the contrast agents was started 9–10 days after the transplantation. Tumor volumes were approximately 50–100 mm^3. The tumor volumes were calculated as follows: volume = $1/2LW^2$; L is the long diameter and W is the short diameter of a tumor.

Twenty-four hours after the injection, the blood was collected with a heparinized syringe and centrifuged at 4 °C for 4 min at 13,000 rpm. The plasma was obtained, and its gadolinium content was measured by means of ICP. The major tissues including tumor tissues were excised and weighted. For the determination of gadolinium ion content in the tissue, saline was added to the tissues, followed by an addition of nitric acid (conc. 70%) and sulfuric acid (conc. 98%). Then, the mixture was heated. A saturated aqueous oxoammonium solution was added to the yellow mixture and heated again. The resulting pale-yellow mixture was diluted with saline. The supernatant was collected, and its gadolinium content was measured by means of ICP. The urine (n = 3) was collected 24 h and 48 h after injection, and its gadolinium content was measured by means of ICP.

2.7. MR imaging of mice tumor model

MR imaging was performed with female mice (CDF_1) bearing a colon 26 tumor. The tumor transplantation was carried out as described in 2.6. The contrast agents were injected at a dose of 0.05 mmol of Gd/kg into a mice-tail vein. MR images were taken with a Varian NMR system at 9.4 T. T_2-weighted fast spin echo (TR = 2500 ms, ETL = 8, ESP = 4, effective TE = 48) was performed for all experiments before following the T_1-weighted gradient echo protocol. T_1-weighted gradient echo protocol was followed before the injection, immediately after the injection, and then 4 h and 24 h after the injection. Imaging parameters of the T_1-weighted images were TR/TE = 8.0/4.2, flip angle = 30°, field of view of 50 × 30 mm, a matrix size of 192 × 192, and 2 mm of coronal slice thickness, and were TR/TE = 8.0/4.5, flip angle = 30°, field of view of 45 × 45 mm, a matrix size of 192 × 192, and 2 mm of axial slice thickness. For normalized signal intensity relative to the T_1-weighted images, the tumor area was selected as a region of interest (ROI). The signal intensity of the ROI was compared with the intensity of a stock solution of 0.1 mM gadolinium ion in agarose gel.

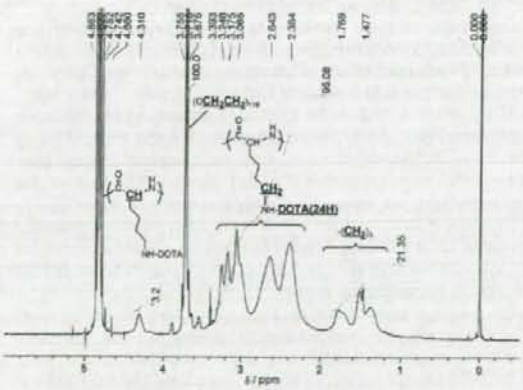

Fig. 2. ^{1}H NMR spectrum of PEG-P(Lys-DOTA) (118-17-17) in D_2O + NaOD.

Please cite this article as: K. Shiraishi, et al., Preparation and in vivo imaging of PEG-poly(L-lysine)-based polymeric micelle MRI contrast agents, J. Control. Release (2009), doi:10.1016/j.jconrel.2009.01.010

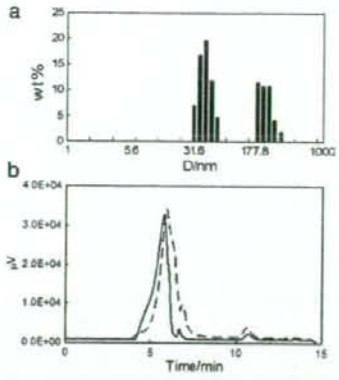

Fig. 3. (a) Weight–weight average size distribution of PEG-P(Lys-DOTA-Gd) micelle (118-17-17-7) in 150 mM NaCl measured by DLS, and (b) gel-permeation chromatogram of PEG-P(Lys-DOTA-Gd) micelle in H_2O (1.2 mg/mL) of concentrated preparation of 118-17-17-7(solid line) and diluted preparation of 118-17-17-6 (dashed line).

The relative signal intensity of the ROI 24 h after the injection was compared with the signal intensity before the injection.

3. Results and discussion

3.1. Block copolymer synthesis and characterization of polymeric micelle

A block copolymer binding DOTA groups was synthesized from poly(ethylene glycol)-*b*-poly(L-lysine). The binding of a DOTA at the lysine residues was carried out with a coupling reaction between a primary amine and an NHS ester of a DOTA reagent, as shown in Fig. 1. Poly(ethylene glycol)-*b*-poly(L-lysine-DOTA) block copolymers possessing 5200 of molecular weights, and 17–21 units of the DOTA-bound lysine moiety were obtained. Quantitative substitution of lysine residues for DOTA was confirmed in ^{1}H NMR spectra as shown in Fig. 2.

A fully DOTA-substituted block copolymer formed polymeric micelles after the dialysis in dist. H_2O at a polymer concentration of 15 mg/mL. The quantitative DOTA conjugation was essential for the polymeric micelle formation. Insufficient DOTA conjugation, such as 118-22-19 wherein the number of DOTA residues was 19 out of 22 lysine residues, did not form a polymeric micelle. This result shows that the micelle structures were not formed in the presence of a small amount of unmodified lysine residue (3 out of 22 residues); the result also underscores the importance of strong interactions among the conjugation DOTA units for the micelle formation.

Gadolinium ion was partially chelated to DOTA in the block copolymer, poly(ethylene glycol)-*b*-poly(L-lysine-DOTA). Gadolinium-chelated poly(ethylene glycol)-*b*-poly(L-lysine-DOTA-Gd) maintained the polymeric micelle formation. Dynamic light scattering (DLS) and GPC measurements of the gadolinium chelated block copolymers, 118-17-17-7 which is 118 ethylene glycol units, 17 lysine residues, 17 DOTA conjugation to lysine residues, and 7 gadolinium ions at DOTA were performed. Fig. 3(a) shows a DLS chart of this block copolymer micelle with a weight average of 42.9±7.6 nm (mean±SD), accompanied by a secondary aggregation of a weight average of 225.5±53.0 nm (mean±SD). Similar secondary aggregation was also found in the precursor of PEG-*b*-poly(L-lysine-DOTA-Gd) (data in supplemental section).

The zeta-potential of the obtained polymeric micelle showed −9.55 mV in 150 mM NaCl solution, indicating that the polymeric micelle was negatively charged. This negative value was given from a vacant DOTA moiety having 3 carboxylic acids and 4 tertiary amines. The tertiary amines of DOTA could work as only two cationic species in the physiological condition owing to their excessively close proximity to each other, whereas three carboxylic acids in the DOTA moiety could work as 3 anions owing to their long distances from one other. As a result, the total charge of the polymeric micelles exhibited negatively charged particles. In general, cationic species are more quickly scavenged by the reticloendothelial system than anionic species [25]. This scavenging is a big obstacle for the passive tumor targeting through the EPR effect. For the design of a tumor-targeting system, a slightly negative-charged particle is preferable as an inert carrier.

GPC measurements of the polymeric micelle (1.2 mg/mL in H_2O) were performed by the use of an HPLC system (LC 2000 series, Jasco, Tokyo, Japan) equipped with a TSK-gel G4000-PW_{XL} column (eluent=H_2O, flow rate=1.0 mg/mL, detector=RI) at 40 °C. Even in such a diluted aqueous solution of the block copolymer, both DLS and GPC measurements clearly exhibit the formation of the polymeric micelle as shown in Fig. 3(b) (solid line). This finding indicated that once the polymeric micelle was formed by interactions among vacant DOTAs, the polymeric micelle was not dissociated in a time scale of a DLS and GPC measurement under dilution. When we injected a similar sample 118-17-17-6 prepared from a dilute condition (3 mg/mL), the peak of the polymeric micelle was shifted to a longer elution time as shown in Fig. 3(b) (dashed line). This result indicates a considerable polymer concentration effect on the formation of the polymeric micelle; namely, strong interactions among vacant DOTA moieties at a high concentration.

Formation of the polymeric micelle with or without a gadolinium ion appears to depend on interactions among vacant DOTAs as described above. To prove this interaction, we added an excess of $GdCl_3$ (2.0 mol equivalent vs DOTA) into 118-20-20 to prepare complete chelation of the DOTA units with gadolinium ions. However, we found that the composition of the block copolymer was 118-20-20-16. Even when we added the excess amount of gadolinium ions to the block copolymer, we obtained 20% of vacant DOTA in the block copolymer. This result implies that DOTA–DOTA interactions prevent gadolinium ion from freely chelating into a DOTA moiety. When we injected this block copolymer into the GPC column, we observed that the peak of around 5–6 min. corresponded to the polymeric micelle disappeared. This disappearance indicates that chelation of a high level of gadolinium ion in a block copolymer resulted in so unstable micelle formation on the GPC column. We concluded that the polymeric micelle was formed through the interactions among vacant DOTAs, and that these interactions depend on the block copolymer concentrations and on the numbers of the chelated gadolinium ions.

3.2. Blood circulation of the polymeric micelle MRI contrast agent

The polymeric micelle, 118-17-17-7, was injected at a dose of 0.05 mmol Gd/kg, into a mouse-tail vein for pharmacokinetic

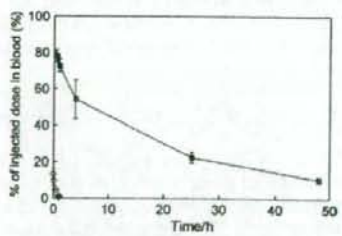

Fig. 4. Blood-concentration time course of PEG-P(Lys-DOTA-Gd) micelle (118-17-17-7) in ddY female mice at a dose of 0.05 mmol Gd/kg (■), and Gd-DTPA at a dose of 0.10 mmol Gd/kg (◇). After defined time periods (0.5 h, 1 h, 2 h, 4 h, 24 h, and 48 h), the blood samples were collected into capillary glass tubes via mice's tail veins.

Please cite this article as: K. Shiraishi, et al., Preparation and in vivo imaging of PEG-poly(L-lysine)-based polymeric micelle MRI contrast agents, J. Control. Release (2009), doi:10.1016/j.jconrel.2009.01.010

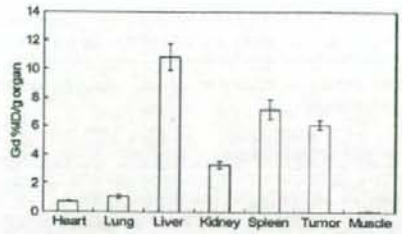

Fig. 5. Biodistribution of PEG-P(Lys-DOTA-Gd) micelle 24 h after injection at a dose of 0.05 mmol Gd/kg.

observations. The blood concentrations of the polymeric micelles were measured by means of ICP. Fig. 4 shows the blood concentration-time course of the polymeric micelles until 48 h after the injection. A low-molecular-weight gadolinium ion complex, such as Gd–DTPA, was immediately excreted 1 h after injection (only 1.4±0.8% was found in blood). On the other hand, the polymeric micelle remained 22.5±2.9% and 10.2±1.4% (mean±SD) in blood at 24 h and 48 h after the injection, respectively. These high blood concentrations exhibit significantly stable circulation of the polymeric micelle in blood. This polymeric micelle underwent an approximately 10-fold dilution relative to the injection in blood: however, stable formation of the polymeric micelle at such diluted conditions was confirmed in this in vivo experiment. This stable blood-circulation time-course was similar to the system of anti-cancer drug-incorporating polymeric micelle, a doxorubicin-incorporating poly(ethylene glycol)-*b*-poly (aspartic acid) system [1]. According to reports, the doxorubicin-incorporating polymeric micelle system provides a drug concentration of 24.6% of the injected dose (ID) after 24 h in the blood. Such a long circulating property of the doxorubicin-incorporating polymeric micelle successfully led to highly selective tumor accumulation. Owing to this similar pharmacokinetic behavior, this MRI contrast agent can be a strong tool for estimation of the pharmacokinetic behavior of "anti-cancer drug"-incorporating polymeric micelles.

3.3. Biodistribution and excretion of the polymeric micelle MRI contrast agent

Selective and high accumulation of drug carriers at solid tumors is essential for an improvement of anticancer drug efficacy. As well as the drug-targeting systems, selective and high accumulation is desired for diagnostic agents.

In recent decades, polymeric micelles have constituted one of the best drug-carriers to have achieved selective accumulation of an anti-cancer drug, through the EPR effect, at solid tumor tissues [1]. Biodistribution of the polymeric micelle contrast agents was evaluated in CDF_1 female mice bearing the colon 26 tumor. Fig. 5 shows the percentage of the injected dose of the polymeric micelle 24 h after the injection in the normal organs as well as in tumor tissues. The study showed that the accumulation of the polymeric micelle contrast agent in tumor tissues reached 6.1±0.3% ID (injected dose)/g of tumor. This accumulation amount was considerably high. Furthermore, highly selective delivery was present with low accumulation amounts in heart, kidney, and muscle tissue. For the mononuclear phagocyte system (MPS), this contrast agent was found to be accumulated in 10.8±0.9 and 7.2±0.7% ID/g of liver and spleen, respectively. These accumulation ratios were similar to those in case of doxorubicin-incorporated polymeric micelle, but better tumor/muscle ratios were obtained in this MRI contrast agent [1]. This difference may rest on a difference in micelle size as well as in detection species: there is a physically entrapped drug for the drug-carrying micelles and there are chelated gadolinium ions for the MRI contrast agent. The gadolinium-binding macromolecular carrier may

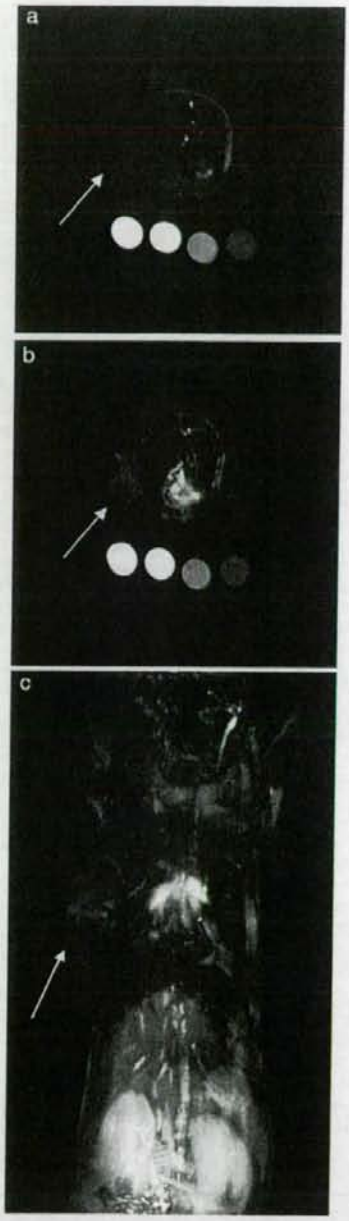

Fig. 6. Axial slices of MR images (a) before and (b) 24 h after the injection at a dose of 0.05 mmol Gd/kg. Tumor areas are on the left side in the axial slices. The circles indicate the stock solutions of (left to right) 1.0 mM, 0.5 mM, 0.1 mM gadolinium ion in agarose gel and blank in agarose gel. T_1-weighted gradient echo protocol was used. Parameters of the T_1-weighted images were TR/TE=8.0/4.5, flip angle=30°, field of view of 45×45 mm, a matrix size of 192×192, and 2 mm of axial slice thickness. Arrows indicate tumor tissue. (c) MIP images of coronal slices 24 h after injection. Arrow indicates tumor. Parameters of the T_1-weighted images were TR/TE=8.0/4.2, flip angle=30°, field of view of 50×30 mm, a matrix size of 192×192. MIP images were obtained by 2 mm thickness×4 slices.

Please cite this article as: K. Shiraishi, et al., Preparation and in vivo imaging of PEG-poly(L-lysine)-based polymeric micelle MRI contrast agents, J. Control. Release (2009), doi:10.1016/j.jconrel.2009.01.010

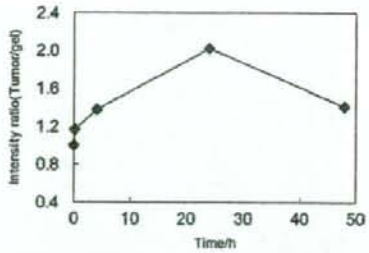

Fig. 7. Relative signal intensities of tumor area at defined time (0 h, 4 h, 24 h, 48 h) after the injection of the polymeric micelle MRI contrast agent.

not penetrate into muscle as do low-"molecular weight" drugs that are released from the carrier.

Wang Y et al. reported that poly[N-(2-hydroxypropyl)methacrylamide] (PHPMA) [14] gadolinium-conjugates exhibited size-dependent tumor accumulation. They stated that a large molecular weight of PHPMA (121 kDa) gadolinium conjugate exhibited the best tumor accumulation at 7 days after injection. Although, Bogdanov A et al. reported another example of successful passive targeting to solid tumors with a graft copolymer of poly(ethylene glycol) featuring poly(L-lysine) [9]. This contrast agent exhibited tumor targeting with a long blood-circulation time ($t_{1/2}$=36 h): however, this long-circulation property in blood indicates that the contrast agent cannot excrete smoothly from the body owing to the polymer's very large molecular weight (690 kDa). The researchers synthesized different molecular weights of similar polymers to compare the polymers' biodistribution [10] and found that the polymers accumulated at solid tumors in a "molecular-weight"-dependent manner. This molecular-weight dependency indicated that smaller molecular weights of polymers can be excreted through the kidneys.

These above-mentioned polymers exhibited better tumor accumulation, corresponded to larger molecular weights of the polymers. However, the excretion of the contrast agent, especially in the case of the macromolecular contrast agent, is a serious matter for the development of diagnostic agents.

Therefore, we checked the kidneys' excretion of our polymeric micelle contrast agent. In urine, 20.8±7.6% of the polymeric micelle was found 48 h after the injection. This result indicates that the polymeric micelle was excreted through the kidney filtration. Since the size of the polymeric micelle contrast agent was 50–250 nm as shown in Fig. 3(a), the polymeric micelles cannot pass through the kidney filtration. Therefore, these polymers that formed in urine appears to have passed through the kidney filtration in a dissociated polymer form, since the average molecular weight of this block copolymer is only 15,000. This is an excellent property of the polymeric micelle MRI contrast agent; namely, this agent exhibits long circulation in blood in a micelle form, while this agent can be excreted through the kidneys in a dissociated polymer form.

Furthermore, the obtained polymeric micelle MRI contrast agent delivered a larger amount to solid tumors than did previously reported macromolecular MRI contrast agents that can be also excreted from the kidneys (agents such as PHPMA gadolinium-conjugate [14] and graft copolymer of poly(ethylene glycol) with poly (L-lysine) [10]).

In order to estimate possible acute toxicity, we injected the 4-fold of the volume of the contrast agent into the mouse tail vein, and observed the body weight change over the course of 16 days. There was no significant difference in comparison to the control (less than ±10%). Although we have to conduct further experiments to obtain toxicity-related information of greater exactness, these preliminary results indicate that this polymeric micelle can dissociate and be excreted from the kidneys, and that this tumor targeting results a passive targeting mechanism (the EPR effect). In a future study, we would like to optimize the pharmacokinetics and the dissociation behavior of the polymeric micelles by controlling the composition of the block copolymers.

3.4. MR imaging at tumor tissue

We took an MR image of the tumor-bearing mouse after the injection of the polymeric micelle contrast agent. Fig. 6 shows T_1-weighted MR images of tumor tissues before and after 24 h at an injection dose of 0.05 mmol Gd/kg. After the injection of the polymeric micelle, MR images exhibited a significant signal enhancement at the kidneys. This signal enhancement at the kidneys indicates that kidneys excreted the contrast agent, as shown in Fig. 6(c). However, even 24 h after the injection, an intense signal was observed in the heart and aorta areas. This indicates that a considerable amount of the contrast agent was circulating in the bloodstream, as described in pharmacokinetic results. The relative signal intensity at axial slices of the tumor tissues underwent a 2.0-fold increase after 24 h, as compared with the signal before the injection. The signal intensity of the tumor area had gradually increased by 24 h and had slightly decreased by 48 h, as shown in Fig. 7. This behavior of the signal intensities is similar to the doxorubicin concentration delivered by the polymeric micelle carrier system. All these results indicate that the enhancement of MR signals in the tumor area rested on the successful passive accumulation of the MRI contrast agent at solid tumors.

4. Conclusion

We prepared polymeric micelle MRI contrast agents using poly (ethylene glycol)-*b*-poly(L-lysine) block copolymers. A reaction of poly(ethylene glycol)-*b*-poly(L-lysine) with a DOTA derivative resulted in a quantitative DOTA conjugation regarding the lysine residues of the block copolymer, and the obtained block copolymer formed a polymeric micelle. This micellar structure was maintained after a partial chelation of the DOTA moiety with gadolinium ions. The biodistribution and the excretion of the polymeric micelle was evaluated in colon 26-bearing CDF_1 female mice. Selective accumulation of the polymeric micelle at the tumor tissues was observed 24 h after the injection. The contrast agent's accumulation substantially enhanced the signal intensity of the MR images at the tumor. This polymeric micelle MRI contrast agent will be a useful diagnostic tool, particularly in combination with a polymeric micelle-based drug-targeting system.

Acknowledgement

This work was supported by the Ministry of Health, Labour, and Welfare of Japan. K. Shiraishi and M. Yokoyama acknowledge the support from the Program for Promoting the Establishment of Strategic Research Centers, Special Coordination Funds for Promoting Science and Technology, the Ministry of Education, Culture, Sports, Science and Technology of Japan, and Tokyo Ohka Foundation for the Promotion of Science and Technology.

Appendix A. Supplementary data

Supplementary data associated with this article can be found, in the online version, at doi:10.1016/j.jconrel.2009.01.010.

References

[1] M. Yokoyama, T. Okano, Y. Sakurai, S. Fukushima, K. Okamoto, K. Kataoka, Selective delivery of adriamycin to a solid tumor using a polymeric micelle carrier system, J. Drug Target. 7 (3) (1999) 171–186.

Please cite this article as: K. Shiraishi, et al., Preparation and in vivo imaging of PEG-poly(L-lysine)-based polymeric micelle MRI contrast agents, J. Control. Release (2009), doi:10.1016/j.jconrel.2009.01.010

[2] Y. Matsumura, H. Maeda, A new concept for macromolecular therapeutics in cancer chemotherapy: mechanism of tumoritropic accumulation of proteins and the antitumor agent Smancs, Cancer Res. 46 (1986) 6387–6392.
[3] H.M. Aliabadi, A. Lavasanifar, Polymeric micelles for drug delivery, Expert Opin. Drug Deliv. 3 (1) (2006) 130–162.
[4] N. Nishiyama, S. Okazaki, H. Cabral, M. Miyamoto, Y. Kato, Y. Sugiyama, K. Nishio, Y. Matsumura, K. Kataoka, Novel cisplatin-incorporated polymeric micelles can eradicate solid tumors in mice, Cancer Res. 63 (2003) 8977–8983.
[5] N. Nishiyama, M. Yokoyama, T. Aoyagi, T. Okano, Y. Sakurai, K. Kataoka, Preparation and characterization of self-assembled polymer–metal complex micelle from cis-dichlorodiammineplatinum(II) and poly(ethylene glycol)-poly(α,β-aspartic acid) block copolymer in an aqueous medium, Langmuir 15 (1999) 377–383.
[6] A. Bogdanov Jr, C. Martin, A.V. Bogdanova, T.J. Brady, R. Weissleder, An adduct of cis-diamminedichloroplatinum(II) and poly(ethylene glycol)poly(L-lysine)-succinate: synthesis and cytotoxic properties, Bioconjug. Chem. 7 (1) (1996) 144–149.
[7] R. Rebizak, M. Schaefer, E. Dellacherie, Polymeric conjugates of Gd^{3+}-diethylenetriaminepentaacetic acid and dextran. 1. Synthesis, characterization, and paramagnetic properties, Bioconjug. Chem. 8 (4) (1997) 605–610.
[8] M.M. Huber, A.B. Staubli, K. Kustedjo, M.H.B. Gray, J. Shih, S.E. Fraser, R.E. Jacobs, T.J. Meade, Fluorescently detectable magnetic resonance imaging agents, Bioconjug. Chem. 9 (2) (1998) 242–249.
[9] A. Bogdanov Jr, S.C. Wright, E.M. Marecos, A.V. Bogdanova, C. Martin, R. Weissleder, A long-circulating co-polymer in "passive targeting" to solid tumors, J. Drug Target. 4 (5) (1997) 321–330.
[10] R. Weissleder, A. Bogdanov Jr, C-H. Tung, H-J. Weinmann, Size optimization of synthetic graft copolymers for in vivo angiogenesis imaging, Bioconjug. Chem. 12 (2) (2001) 213–219.
[11] F. Ye, T. Ke, E-K. Jeong, X. Wang, Y. Sun, M. Johnson, Z-R. Lu, Noninvasive visualization of in vivo drug delivery of poly(L-glutamic acid) using contrast-enhanced MRI, Mol. Pharm. 3 (5) (2006) 507–515.
[12] X. Wen, E.F. Jackson, R.E. Price, E.E. Kim, Q. Wu, S. Wallace, C. Charnsangavej, J.G. Gelovani, C. Li, Synthesis and characterization of poly(L-glutamic acid) gadolinium chelate: a new biodegradable MRI contrast agent, Bioconjug. Chem. 15 (6) (2004) 1408–1415.
[13] Z-R. Lu, X. Wang, D.L. Parker, K.C. Goodrich, H.R. Buswell, Poly(L-glutamic acid) Gd (III)–DOTA conjugate with a degradable spacer for magnetic resonance imaging, Bioconjug. Chem. 14 (4) (2003) 715–719.
[14] Y. Wang, F. Ye, E-K. Jeong, Y. Sun, D.L. Parker, Z-R. Lu, Noninvasive visualization of pharmacokinetics, biodistribution, and tumor targeting of poly[N-(2-hydroxypropyl)methacrylamide] in mice using contrast enhanced MRI, Pharm. Res. 24 (6) (2007) 1208–1216.
[15] H. Kobayashi, M.W. Brechbiel, Dendrimer-based macromolecular MRI contrast agents: characterization and application, Mol. Imag. 2 (1) (2003) 1–10.
[16] H. Kobayashi, S. Kawamoto, S-K. Jo, H.L. Bryant Jr, M.W. Brechbiel, R.A. Star, Macromolecular MRI contrast agents with small dendrimers: pharmacokinetic differences between sizes and cores, Bioconjug. Chem. 14 (2) (2003) 388–394.
[17] H. Kobayashi, N. Sato, S. Kawamoto, T. Saga, A. Hiraga, T.L. Haque, T. Ishimori, J. Konishi, K. Togashi, M.W. Brechbiel, Comparison of the macromolecular MR contrast agents with ethylenediamine-core versus ammonia-core generation-6 polyamidoamine dendrimer, Bioconjug. Chem. 12 (1) (2001) 100–107.
[18] E. Nakamura, K. Makino, T. Okano, T. Yamamoto, M. Yokoyama, A polymeric micelle MRI contrast agent with changeable relaxivity, J. Control. Release 114 (2006) 325–333.
[19] V.P. Torchilin, PEG-based micelles as carriers of contrast agents for different imaging modality, Adv. Drug Deliv. Rev. 54 (2002) 235–252.
[20] G. Zhang, R. Zhang, X. Wen, L. Li, C. Li, Micelles based on biodegradable poly(L-glutamic acid)-b-polylactide with paramagnetic Gd ions chelated to the shell layer as a potential nanoscale MRI-visible delivery, Biomacromolecules 9 (1) (2008) 36–42.
[21] H.Y. Lee, H.W. Jee, S.M. Seo, B.K. Kwak, G. Khang, S.H. Cho, Diethylenetiramine-pentaacetic acid–gadolinium (DTPA–Gd)-conjugated polysuccinimide derivatives as magnetic resonance imaging contrast agents, Bioconjug. Chem. 17 (3) (2006) 700–706.
[22] N. Nasongkla, E. Bey, J. Ren, H. Ai, C. Khemtong, J.S. Guthi, S-F. Chin, A.D. Sherry, D.A. Boothman, J. Gao, Multifunctional polymeric micelles as cancer-targeted, MRI-ultrasensitive drug delivery systems, Nano Lett. 6 (11) (2006) 2427–2430.
[23] Z-R. Lu, F. Ye, A. Vaidya, Polymer platforms for drug delivery and biomedical imaging, J. Control. Release 122 (2007) 269–277.
[24] M. Yokoyama, G.S. Kwon, T. Okano, Y. Sakurai, M. Naito, K. Kataoka, Influencing factors on in vitro micelle stability of adriamycin-block copolymer conjugate, J. Control. Release 28 (1994) 59–65.
[25] Y. Takakura, T. Fujita, M. Hashida, H. Sezaki, Disposition character of macromolecules in tumor-bearing mice, Pham. Res. 7 (4) (1990) 330–346.
[26] A. Harada, K. Kataoka, Formation of polyion complex micelles in an aqueous milieu from a pair of oppositely-charged block copolymers with poly(ethylene glycol) segments, Macromolecules 28 (15) (1995) 5294–5299.

Please cite this article as: K. Shiraishi, et al., Preparation and in vivo imaging of PEG-poly(L-lysine)-based polymeric micelle MRI contrast agents, J. Control. Release (2009), doi:10.1016/j.jconrel.2009.01.010

Journal of Controlled Release xxx (2009) xxx–xxx

Contents lists available at ScienceDirect

Journal of Controlled Release

journal homepage: www.elsevier.com/locate/jconrel

NANOMEDICINE

Histological study on side effects and tumor targeting of a block copolymer micelle on rats

Takanori Kawaguchi [a,b], Takashi Honda [b], Masamichi Nishihara [c], Tatsuhiro Yamamoto [c], Masayuki Yokoyama [c,*]

[a] Department of Pathology, Aizu Central Hospital, Aizu Wakamatsu 965-8611, Japan
[b] Division of Human Life Sciences, Fukushima Medical University School of Nursing, Hikariga-oka 1, Fukushima, Fukushima 960-1295, Japan
[c] Yokoyama Project, Kanagawa Academy of Science and Technology, KSP East 404, Sakado 3-2-1, Takatsu-ku, Kawasaki, Kanagawa 213-0012, Japan

ARTICLE INFO

Article history:
Received 11 September 2008
Accepted 12 February 2009
Available online xxxx

Keywords:
Polymeric micelle
Pathology
Side effects
Block copolymer
Targeting

ABSTRACT

Histological examinations were performed with polymeric micelle-injected rats for evaluations of possible toxicities of polymeric micelle carriers. Weight of major organs as well as body weight of rats was measured after multiple intravenous injections of polymeric micelles forming from poly(ethylene glycol)-b-poly (aspartate) block copolymer. No pathological toxic side effects were observed at two different doses, followed only by activation of the mononuclear phagocyte system (MPS) in the spleen, liver, lung, bone marrow, and lymph node. This finding confirms the absence of – or the very low level of – in vivo toxicity of the polymeric micelle carriers that were reported in previous animal experiments and clinical results. Then, immunohistochemical analyses with a biotinylated polymeric micelle confirmed specific accumulation of the micelle in the MPS. The immunohistochemical analyses also revealed, first, very rapid and specific accumulation of the micelle in the vasculatures of tumor capsule of rat ascites hepatoma AH109A, and second, the micelle's scanty infiltration into tumor parenchyma. This finding suggests a unique tumor-accumulation mechanism that is very different from simple EPR effect-based tumor targeting.

1. Introduction

Recently, block copolymer micelles have gained considerable attentions as an efficacious carrier system of anti-cancer drugs [1–4]. Two objectives have been pursued with the polymeric micellecarriers: solubilization of water-insoluble drugs and targeting to solid tumors. Owing to a large loading capacity of the polymeric micelles' inner core for hydrophobic drugs, the polymeric micelles facilitate easy and safe intravenous injections of water-insoluble drugs such as paclitaxel [5,6]. The second objective, the targeting of the polymeric micelle carrier systems to solid tumors, is achieved by the targeting through the EPR (enhanced permeability and retention) effect [7,8]. For effective utilization of the EPR effect, poly(ethylene glycol) (PEG) has been used as an outer-shell-forming polymer block owing to its inert characteristics in interactions and uptake with or by bio-components such as proteins and cells. In particular, the PEG outer shell of the micelle is considered a critical factor in the reduction of micelle uptake by the mononuclear phagocyte system (MPS). For several anti-cancer drugs such as doxorubicin [2], cisplatin [9], and paclitaxel [10], the tumor targeting was successfully achieved in solid-tumor models in mouse. Research reported that, accompanying this targeting effect were diminished toxic side effects of the incorporated anti-cancer drugs: specifically, a reduction of nephrotoxicity [11] and pulmonary toxicity [12]. Furthermore, a paclitaxel-incorporating polymeric micelle enhanced the radiosensitizing activity of the drug [13]. Following these good results in animal evaluations, four clinical trials of polymeric micelle targeting are underway in 2008 for doxorubicin [14] paclitaxel [15], cisplatin [9], and SN-38 [16,17], the last of which is an active species of CPT-11.

The targeting efficiency and the toxic side effects of a given carrier are two important issues for drug targeting. In the "animal-tumor model" studies and the clinical-trial results mentioned above, carrier-based toxicities were not observed. In other words, the conclusion was that all the observed toxic side effects in animals and humans had resulted from either the anti-cancer drug delivered to normal organs and tissues or the drug released from the polymeric micelle carrier during its circulation in the bloodstream. Research has frequently noted the presence of carrier-based toxic side effects in drug targeting systems, and these side effects have included the hand–foot syndrome for a doxorubicin-incorporating liposome [18] and the infusion-related reactions for an antibody–anti-cancer drug conjugate [19]. These adverse effects can be a major concern in their clinical uses. Therefore, no or low toxicity in the polymeric micelle carriers seems a great advantage. Although the polymeric micelle systems are considered

* Corresponding author. Tel.: +81 44 819 2093; fax: +81 44 819 2095.
E-mail address: yp-yokoyama2093ryo@newkast.or.jp (M. Yokoyama).

0168-3659/$ – see front matter © 2009 Published by Elsevier B.V.
doi:10.1016/j.jconrel.2009.02.011

Please cite this article as: T. Kawaguchi et al., Histological study on side effects and tumor targeting of a block copolymer micelle on rats, J. Control. Release (2009), doi:10.1016/j.jconrel.2009.02.011

very safe carriers at least for anti-cancer drugs, it is worth while to conduct detailed histological and immunohistological examinations to identify the exact profiles and the exact mechanisms of the polymeric micelle carriers' possible toxic side effects. It is believed that these examinations can contribute not only to increasingly refined polymeric micelle designs for anti-cancer drug targeting, but also to polymeric micelles' applications to drugs other than anti-cancer drugs. In general, non-anti-cancer drugs exhibit milder toxic side effects than anti-cancer drugs. Even if carriers possess a low level of toxic side effects, these side effects may not be detected in the presence of strong toxic side effects of anti-cancer drugs. In such circumstance, it is not so important to examine the carriers' toxic effects in detail. In contrast, the carriers' toxic effects may be easily detected and be a problem in carriers' applications to non-anti-cancer-drugs that exhibit much milder side effects than anti-cancer drugs. Therefore, greater details in carriers' toxicity observation may be required for drug carriers' application to the non-anti-cancer drugs.

Concerning in vivo activities of polymeric micelles or of micelle-forming block copolymers, two interesting phenomena were reported: the depletion-of-ATP phenomenon and ABC (accelerated blood clearance) phenomenon. Kabanov et al. reported that Pluronic block polymers (poly(ethylene oxide)-b-poly(propylene oxide)-b-poly(ethylene oxide) block copolymers) could inhibit the activity of the protein playing a major role in multi-drug resistance through an ATP depletion mechanism [20,21]. The second ABC phenomenon is that clearance of long-circulating drug carriers is enhanced at the second dose through an immunological action. This phenomenon was reported by Dams et al. [22] and by Ishida et al. [23,24] for PEG-coated liposomes. Recently, this ABC phenomenon was also observed for a polymeric micelle carrier [25]. Therefore, it is challenging and interesting to examine detailed biological activities of PEG-based polymeric micelles whose distinctive activities or toxicities cannot be found in simple in vivo tests. No histological examinations, however, have been conducted for the polymeric micelle carriers that do not load any drug.

The current study analyzes acute biological activities of polymeric micelles forming from poly(ethylene glycol)-b-poly(aspartate) block copolymers that achieved successful tumor targeting of an anti-cancer agent camptothecin [26,27] and targeting of all-trans retinoic acid [28] by incorporation of these agents into the micelle. In this study, a term 'acute' is used to indicate a term of several weeks after the micelle injection. Therefore, the biological analysis is carried out for 30 days in the longest case. This study measured weight change of the whole body and major organs, and preformed histopathological observations with rats. Furthermore, a biotinylated polymeric micelle was prepared, and its

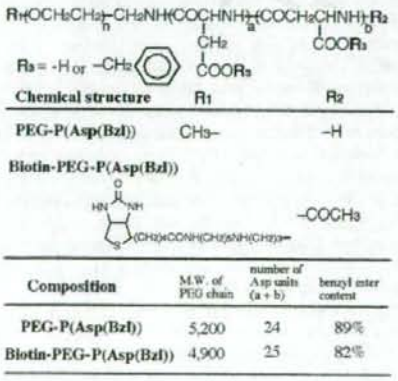

Composition	M.W. of PEG chain	number of Asp units (a + b)	benzyl ester content
PEG-P(Asp(Bzl))	5,200	24	89%
Biotin-PEG-P(Asp(Bzl))	4,900	25	82%

Fig. 1. Chemical structures and compositions of PEG-P(Asp(Bzl)) and biotin-PEG-P(Asp (Bzl)) block copolymers.

Table 1
Weights of major organs after polymeric micelle injections

Dose	20 mg/kg×5[a]			200 mg/kg×5[b]		
	Polymeric micelle	Control[c]	Statistical significance[d]	Polymeric micelle	Control[c]	Statistical significance[d]
Brain	1.36±0.06	1.35±0.09	n.s.[e]	1.65±0.10	1.57±0.10	n.s.[e]
Heart	0.95±0.09	0.89±0.09	n.s.	0.58±0.06	0.67±0.07	n.s.
Lung	1.33±0.11	1.27±0.19	n.s.	121±0.08	1.44±0.12	n.s.
Liver	18.18±1.47	16.80±2.09	n.s.	10.60±1.08	10.55±0.67	n.s.
Spleen	0.70±0.09	0.64±0.10	n.s.	0.37±0.06	0.46±0.07	n.s.
Kidney	247±0.20	2.39±0.16	n.s.	1.61±0.16	1.73±0.16	n.s.

[a] Injections on days 0,1,3,5, and 7. Weights of organs were measured on day 30.
[b] Injections on days 0,1,2,3, and 4. Weights of organs were measured on day 7.
[c] Injections of physiological saline.
[d] By Student's *t*-test. Difference is considered significant when $p<0.05$.
[e] n.s.: not significant.

tissue/cell distribution was analyzed with tumor-bearing rats. These evaluations and analyses provide valuable information on toxicity profiling of the polymeric micelle carriers, and may yield deep insight into polymeric micelles' targeting mechanism at solid-tumor sites.

2. Materials and methods

2.1. Preparation of block copolymer micelle

Two block copolymers were synthesized. Their chemical structures are shown in Fig. 1. One block copolymer is poly(ethylene glycol)-block-poly(aspartate) (PEG-P(Asp(Bzl)), which possesses both a hydrophilic aspartic acid residue and a hydrophobic benzyl aspartate residue in one polymer block. This block copolymer was synthesized according to a previously reported method [29]. As summarized in Table 1, the PEG chain's average molecular weight of this block copolymer was 5200, and the average number of the Asp units was 24. The benzyl ester content was 89% with respect to the Asp unit. The other block copolymer is biotinyl-poly(ethylene glycol)-block-poly (benzyl aspartate) (biotin-PEG-P(Asp(Bzl)), which possesses almost the same composition as that of PEG-P(Asp(Bzl) except that the former features the terminal biotin moiety. In the current study, this biotinylated polymer was prepared according to the same method [29] with some modifications in the biotinylation at a polymer terminal. The starting material for this synthesis was α-amino propyl-ω-3,3-diethoxypropyloxy poly(ethylene glycol) (acetal-PEG-NH_2). The average molecular weight of this PEG block was 4900. Detailed synthetic procedures will be published elsewhere. In brief, the biotinylation was conducted according to a Schiff-base formation between the terminal aldehyde group and a biotinylation reagent, 5-(biotinamido)pentylamine (Pierce Biotechnology, Inc., Rockford, IL). The formed Schiff-base was reduced with sodium cyanoborohydride to obtain a stable secondary amine group as shown in Fig. 1. The obtained biotin-PEG-P(Asp(Bzl)) was characterized by means of ^{1}H NMR spectroscopy. From a ^{1}H NMR spectrum, conjugation of the biotin residue at the polymer terminal was found quantitatively (104%), and the benzyl ester content at the aspartic acid residue was determined to be 82%. The number of the aspartic acid residue was 25, and the molecular weight of this biotin-PEG-P (Asp(Bzl)) was 9700, as summarized in Fig. 1.

A polymeric micelle solution was prepared by means of a solvent-evaporation method as described previously [17]. The block copolymer was dissolved in chloroform. The solution was stirred in a glass bottle under a dry N_2 flow, allowing for evaporation of chloroform. Then, water was added to the dried residue, and sonication was applied so that a dispersed micelle solution would result. "Block copolymer micelle" solutions were stored at −30 °C until use. In non-biotinylated polymeric micelle preparations for toxicity evaluations, PEG-P(Asp(Bzl)) was used. In biotinylated micelle preparations, 10 mol% of biotin-PEG-P(Asp(Bzl)) and 90 mol% of (non-biotinylated)

Please cite this article as: T. Kawaguchi et al., Histological study on side effects and tumor targeting of a block copolymer micelle on rats, J. Control. Release (2009), doi:10.1016/j.jconrel.2009.02.011

PEG-P(Asp(Bzl)) (molecular weight of the PEG chain: 5200, number of Asp units: 24, benzyl ester content: 89%, and total molecular weight: 9800) were mixed and applied to the evaporation method.

2.2. Animal tests

2.2.1. Animals

Four-week-old to six-week-old female Donryu strain rats (60–80 g) were purchased from Chares River (Tokyo, Japan). The rats were maintained under water ad libitum and were used for experiments when they grew to 120–160 g. All animal experiments were carried out under the control of the Animal Research Committee in accordance with both the Guidelines on Animal Experiments in Fukushima Medical University, School of Medicine and the Japanese Government Animal Protection and Management Law.

2.2.2. Experimental design

Three types of experiments were carried out as stated below.

(1) Low-dose experiment
Rats received intravenous (i.v.) injections through a tail vein at a dose of 20 mg polymeric micelle/kg body weight in 0.5 ml physiological saline per day 5 times on days 0, 1, 3, 5, and 7. The micelle for the injection was formed from (non-biotinylated) PEG-P(Asp(Bzl)). The control rats received the same volume of physiological saline. Body weights of these rats were measured every other day until day 30. Six rats were used for the micelle-injected group, and six other rats were used for the control group. The rats were sacrificed on day 30 under deep ether anesthesia, and the weights of the brain, heart, lungs, liver, spleen, and kidneys were measured. The major organs and tissues (brain, thymus, lymph node, heart, lungs, liver, spleen, gastro-intestines, pancreas, kidneys, adrenal gland, ovary, uterus, muscle, and bone) were removed and were fixed in 10% formalin. These samples were processed for hematoxylin and eosin (HE) staining according to the standard method.

(2) High dose experiment
Rats received i.v. injections of a polymeric micelle at a dose of 200 mg polymeric micelle/kg body weight in 0.5 ml physiological saline per day 5 times at days 0, 1, 2, 3, and 4 and were sacrificed on day 8. The micelle for injection was formed with (non-biotinylated)PEG-P(Asp(Bzl)). The control rats received the same volume of physiological saline. The body weights of these rats were measured every day until day 7. Six rats were used for the micelle-injected group and the control group, each. Measurements of organ weights and their histological examinations were performed in the same manners as those for the low-dose experiment as described above.

(3) Histological observation with tumor-bearing rat
Rat ascites hepatoma AH109A cells [30], 4×10^6 cells/0.5 ml physiological saline, were inoculated, specifically in the subcutaneous tissues of the abdominal walls of 10 rats on day 0. Two rats received i.v. with 10 mg biotinylated micelles dispersed in 1 ml of physiological saline on day 2 and day 3 and were sacrificed 1 h and 1 day after the injection, respectively. This dose corresponds to approx. 60–80 mg/kg. On day 7, 6 rats received i.v. with 10 mg biotinylated micelles in 1 ml physiological saline. Two rats were sacrificed 1 h later, and other two rats were sacrificed 1 day later, and two other rats were sacrificed 1 week later. On day 14, two rats received i.v. with 10 mg biotinylated micelles. One rat was sacrificed 1 h later, and the other one was sacrificed 1 day later. All rats were sacrificed under deep ether anesthesia followed by Nembutal (pentobarbital sodium) anesthesia with circulation of physiological saline of 50–100 ml from the left ventricle to the right atrium.

2.3. Histology and immunohistochemistry

Histological materials were fixed in 10% formalin and embedded in paraffin, and then sections with 3 μm thickness were prepared. These thin sections were placed on glass slides, deparaffined in xylen, and dehydrated in graded alcohols. These slides were stained with hematoxylin and eosin (HE). Immunohistochemistry was performed according to a streptavidin–biotin complex method as described previously [31]. Briefly, endogenous peroxidase was blocked in 0.3% H_2O_2 in 100% methanol for 10 min. Some slides were sonicated for 10 min in a citrate buffer, pH 6.0. So that there would be a reduction in the nonspecific binding of the primary antibodies, sections were preincubated for 20 min at room temperature in 2% bovine serum albumin (BSA, Sigma, St. Louis, MO, USA). After washing with PBS, slides were covered with primary antibodies described below for overnight at 4 °C. Incubation with biotinylated secondary antibodies (Nichirei, Tokyo, Japan) was done at room temperature for 30 min. We applied a streptavidin–biotin–peroxidase complex (Nichirei, Tokyo, Japan or Vector Laboratories, Burlingame, CA, USA) to each slide. Binding was detected by hydrogen peroxidase/3,3′-diaminobenzidine tetrahydrochloride (DBA, Dojindo, Kumamoto, Japan). Hematoxylin was used for counterstaining. Sections with known expression of the respective epitope were used as positive controls, whereas the primary antibody was replaced with an antibody-dilution solution, serving as negative controls.

An anti-rat CD68 mouse monoclonal antibody was purchased from HyCult biotechnology b.v. (Uden, Netherlands). The antibody of 1 μg/100 μl PBS was applied to every slide. The mouse anti-biotin monoclonal antibody was purchased from Roche Diagnostic GmbH (Penzberg, Germany). The antibody of 1 μg/100 μl PBS was applied to every slide.

2.4. Statistical analysis

Data between groups were compared by means of Student's *t*-test. Differences were considered to be significant when $p<0.05$.

3. Results

3.1. Toxicity examinations

In the low-dose experiment (20 mg polymer/kg), the average body weight of the micelle-injected group was compared with that of the control group. As shown in Fig. 2, there was no statistically significant difference in body weights between the two groups although the micelle-injected group was slightly lighter than the control prior to the first injection. The weights of the brain, heart, lungs, liver, spleen, and kidneys of micelle-group rats did not differ from those of the control group as summarized in Table 1. No particular pathological

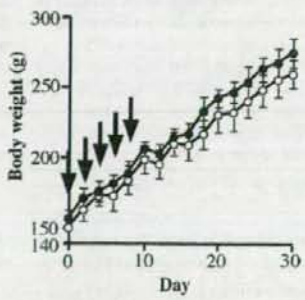

Fig. 2. Body-weight change in rats that received 20 mg/kg micelle or physiological saline 5 times (at arrows). No statistically significant differences were found between the micelle group and the control group.

Please cite this article as: T. Kawaguchi et al., Histological study on side effects and tumor targeting of a block copolymer micelle on rats, J. Control. Release (2009), doi:10.1016/j.jconrel.2009.02.011

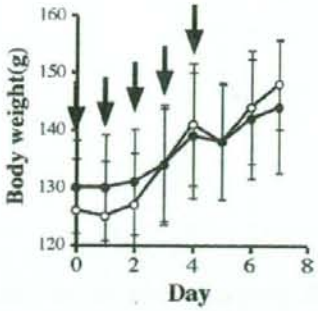

Fig. 3. Body-weight change in rats that received 200 mg/kg micelle or physiological saline 5 times at arrows. No statistically significant differences were found between the micelle group and the control groups.

changes were found in all these examined organs and tissues including bone marrow. Foamy cells were found focally in the lungs and lymph nodes in some rats as shown in Fig. 4a and c, respectively. Foamy-cell accumulation was observed in the lungs and the lymph nodes of the control group, but the degrees were milder than those of the micelle groups as shown in Fig. 4b and d.

Since no toxicity was observed in the low-dose experiment as stated above, a further pathological examination was carried out with an injected dose raised to 200 mg/kg so that there could be an accurate determination of any possible side effect of the micelle. The micelle was intravenously injected at 200 mg polymer/kg 5 times every day into rats, followed by (1) detailed examinations of body weight and organ weight, and (2) histology of organs/tissues. As shown in Fig. 3 and Table 1, there were no differences in the average body weight and in the average organ weight of rats between the micelle-treated group and the control group. In histological observations of HE sections, no abnormality was found in most examined organs and tissues.

One marked change in the micelle-treated group was seen: an increase of foamy cells in the spleen. This increase was observed in all treated rats as shown in Fig. 4e. This finding shows a clear contrast between the spleen of the micelle-injected group (Fig. 4e) and the spleen of the control (Fig. 4f). Staining with the anti-rat CD68 monoclonal antibody confirmed that the foamy cells were macrophages, as shown in Fig. 4g. Immunohistological examinations revealed marked increases in CD68-positive macrophages in the spleen, liver, lymph node, and lungs of the micelle-injected group when these sections were compared with those of the control group (Fig. 4g, i, and k for the rat injected with the micelle and Fig. 4h, j, and l for the control group.). The increase was much more dramatic in the spleen than in the liver and the lungs. The CD-68 immunohistological examination in lymph node was

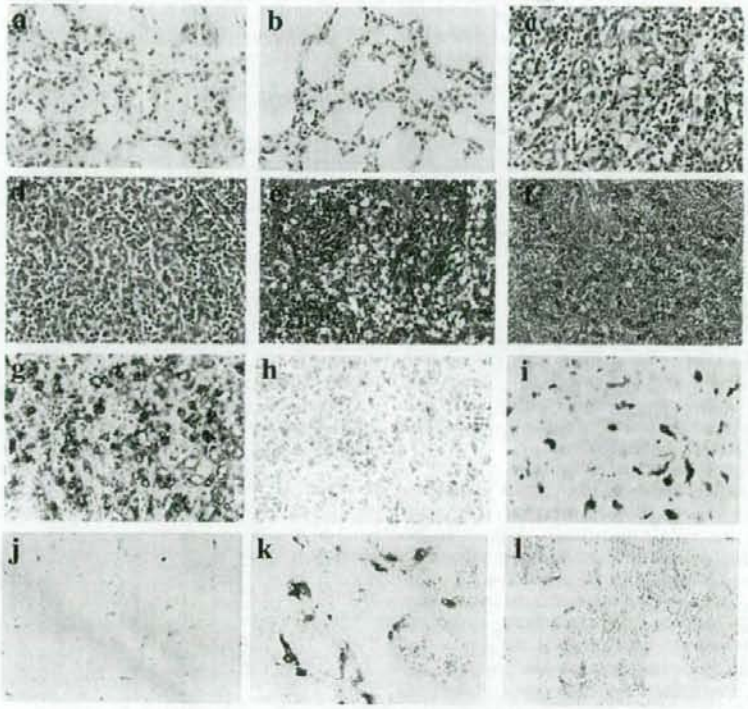

Fig. 4. Histological and immunohistochemical demonstrations of activated MPS in rats that received the micelle. ×400 in the original. (a)–(f): HE staining, and (g)–(l): immunostaining with mouse anti-rat CD68 monoclonal antibody. (a) and (c): accumulation of foamy cells in the lungs and lymph nodes, respectively, belonging to rats that received 20 mg/kg×5 times and were sacrificed at 30 days after the first injection of the micelle. (b) and (d): lungs and lymph nodes of the control groups, respectively. Foamy-cell accumulation was observed in the lungs and the lymph nodes of the control group, but the degrees were milder than those of the micelle groups. (e): foamy cells in the spleen. Foamy cells were accumulated in the spleens belonging to all rats that received 200 mg/kg×5 times and were killed at 7 days after the first injection of the micelle. (f): foamy-cell accumulation was rarely found in the spleen of control rats. Here is an immunohistochemical demonstration of activated MPS in (g) the spleen, (i) the liver, and (k) the lungs of the micelle-injected rats. Control mice exhibited smaller numbers of immunostaining-positive cells in (h) the spleen, (j) the liver, and (l) the lungs.

Please cite this article as: T. Kawaguchi et al., Histological study on side effects and tumor targeting of a block copolymer micelle on rats, J. Control. Release (2009), doi:10.1016/j.jconrel.2009.02.011

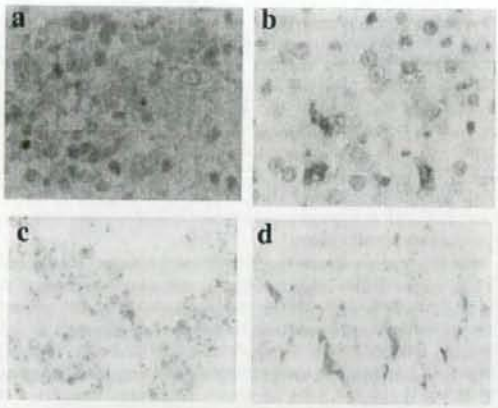

Fig. 5. Immunohistochemistry-based demonstration of biotinylated micelles. Anti-biotin antibody-positive signs were found on mononuclear cells in (a) the spleen, (b) the liver (Kupffer cells), and (c) the lungs (alveolar macrophage). Biotin-positive signs were also found in (d) renal tubules. These tissues were taken from a rat that bore a 2-week-old tumor and that had been sacrificed 24 h after the i.v. injection of 10 mg of biotinylated micelle / rat.

not done. From their intra-sinusoidal location and features, the foamy cells in the liver appeared to be Kupffer cells.

3.2. Microscopic observation of biotynylated micelle disposition with tumor-bearing rats

For immunohistological examinations, a biotinylated micelle was prepared (its chemical structure is shown in Fig. 1) for clarification of the micelle's accumulation behavior in tumor-bearing rats. One hour after the i.v. injection, no sign of the biotinylated micelle accumulation was found in most organs and tissues, including the spleen, liver, lungs, and lymph nodes. In contrast, biotinylated micelle-positive signs were found in the mononuclear phagocyte system (MPS) of the spleen, liver (Kupffer cells), and lungs 1 day after the injection, as shown in Fig. 5a–c. In addition, micelle accumulation was found in intra-tubules of kidneys (Fig. 5d). The biotinylated micelles were detected clearly in the MPS of the liver 1 week after the injection. (data not shown).

Disposition of the biotinylated micelle at the AH109A tumor was observed. As shown in Fig. 6a, the biotinylated micelle accumulation was evident as early as 1 h after injection in the blood vessels of the tumors that were transplanted 2 weeks before the micelle injection. This is a very interesting phenomenon because 1 h is a much shorter period than those are generally argued in targeting of the long-circulating drug carrier systems (e.g., PEG-coated liposomes and polymeric micelles) that utilize the EPR effect as a passive targeting strategy. It was reported that these long-circulating drug carrier systems provided the maximum delivery amounts at the tumor tissues 24 or 48 h post intravenous injection [18,33]. This unique and speedy micelle accumulation was also observed in younger 2-day-old and 1-week-old tumors. (The current study analyzed these tumors 2 days and 1 week after the tumor transplantation.) (data not shown) In enlarged images (Fig. 6b and c), most of the biotin-positive images were found in a highly concentrated manner. As shown in Fig. 6d, an elastic fiber staining image clearly indicates this is an arterial blood vessel.

This finding suggests that the observed micelles were aggregates of the micelles, not dispersed micelles. However, this issue needs further examination for confirmation of the observation in question.

The current study conducted this immunohistological examination both in the peripheral areas and the central areas of the tumor. Fig. 7a and b shows the immunohistological images of the peripheral and central parts, respectively. As shown in Fig. 7a for a 2 week-old tumor-bearing rat, the micelles were clearly observed in the blood vessels of the tumor capsule 1 day after the micelle injection. The micelles were also observed in the tumor parenchyma (tumor cells, tumor interstitium of blood vessels, and fibrous tissue) The range of tumor parenchyma which showed the micelle-positive signs was approximate 200 μm, and the micelle-positive signs in the tumor parenchyma showed smaller and finer granular appearance than the micelle-positive signs in the capsular blood vessels. Fig. 7b shows that the micelles were also observed in the dilated and distorted blood vessels of the central tumor area, and that fine granular micelle-positive deposits were found in tumor cells neighboring to these blood vessels. This image was obtained 1 week after the i.v. injection of the micelle. These findings suggest that the observed micelles in the blood vessels were the aggregates of the micelles, while the micelles in the tumor parenchyma were the dispersed micelles. It is commonly accepted that delivery to a tumor's central area is very difficult owing to several inhibitory issues such as high interstitial pressure. In fact, the first paper concerning the EPR effect reported that macromolecules' delivery to the central area was much less effective than the delivery to the peripheral area [7] Therefore, this micelle accumulation in the center area is interesting. The micelles were not clearly observed in extravascular space also in the case where the micelle accumulated in the central area of the tumor.

4. Discussion

The polymeric micelle drug carrier system is advantageous for a container of hydrophobic drugs owing to the hydrated micelle outer

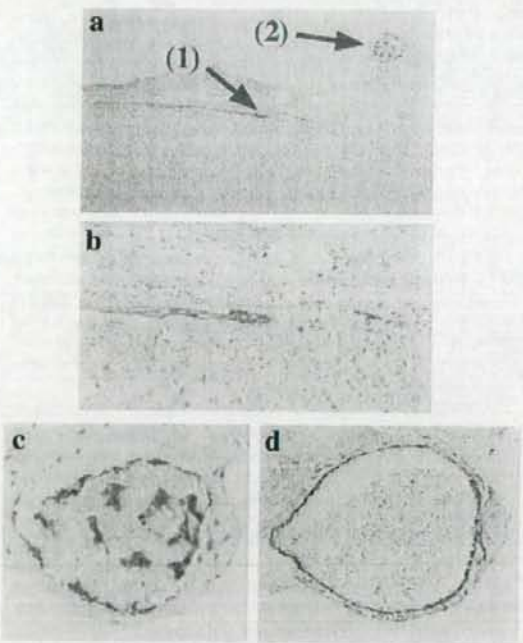

Fig. 6. Tumor targeting of biotinylated micelles. A rat with a 2-week-old tumor was injected with biotinylated micelles and was sacrificed under circulation of 100 ml physiological saline 1 h after the injection. (a) Blood vessels of peri-tumor connective tissues (capsule of tumor) exhibited strong anti-biotin antibody-positive signs. (b) Enlargement of arrow (1). The blood vessel seemed to be a capillary. (c) Enlargement of arrow (2). Anti-biotin antibody-positive signs were found along a blood-vessel surface in addition to a surface of a mass in the blood vessel. Some of the positive signs were seen in the blood. (d) Elastic fiber staining of panel c. This staining indicates that this is an arterial blood vessel.

Please cite this article as: T. Kawaguchi et al., Histological study on side effects and tumor targeting of a block copolymer micelle on rats, J. Control. Release (2009), doi:10.1016/j.jconrel.2009.02.011

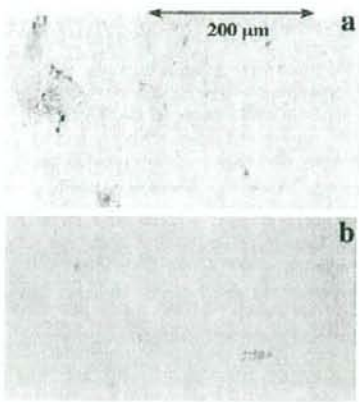

Fig. 7. Immunohistochemical observation of polymeric micelles at different areas of the tumor. (a) The micelles appeared in blood vessels of the tumor peripheral area. The material was taken from a 2-week-old-tumor 1 day after the i.v. injection of biotinylated micelle. The micelles appeared in the blood vessels of the tumor peripheral area (tumor capsule) and tumor parenchyma (tumor cells and tumor blood vessels) near the tumor capsule. (b) The micelles were detected in tumor blood vessels in the center area of the tumor 1 week after the i.v. injection into the 1-week-old-tumor. The micelles were detected in dilated and irregular-shaped blood vessels in center areas of the tumor 1 week after the i.v. injection into the 1-week-old tumor, where necrosis and degeneration occurred. The micelles were also detected in intact tumor cells around such blood vessels.

shell, which can effectively inhibit precipitation caused by hydrophobicity of the incorporated drug. In addition, the block copolymer micelle incorporating anti-cancer drug can accumulate selectively at tumor tissues by means of the EPR effect [7,8,32]. No studies have closely examined biological activities related to possible toxic side effects of the polymeric micelle carriers, although in vivo results for anti-cancer drug polymeric micelles suggested no or very low carrier-related toxicities. Concerning the EPR effect's selective accumulation, many reports have supported this EPR effect-based targeting strategy; nevertheless, several fundamental questions remain unelucidated: What parts of tumor tissues and vasculatures are the most active in exhibiting the EPR effect? How quick is permeation of polymeric micelles in tumor interstitium? And how dependent are the above-stated phenomena on the size of polymeric micelles? The authors have developed the PEG-P (Asp(Bzl)) micelle for anti-cancer drug targeting [26,27,29]. Using this PEG-P(Asp(Bzl)) micelle, the present study conducted the first detailed examinations of the acute in vivo effects of a polymeric micelle carrier.

The current study detected no toxic side effects of the micelle in any examined organs/tissues, even in cases where there was a large injection dose of the micelles (200 mg/kg×5). There was only one marked change in a micelle-treated rat: the activation of the mononuclear phagocyte system (MPS); also, the micelle exhibited a high accumulation in the MPS of the spleen, lungs, lymph node, and liver (Kupffer cells). This study constitutes the first report histologically demonstrating the accumulation of block copolymer micelles in the MPS in vivo. This activation is not a pathological change, but may be important to immunological reactions such as the ABC phenomenon [22–25]. Previous research reported that the polymeric micelle carrier system accumulated in the liver at a higher concentration than in other normal organs, and that the accumulated micelle remained present in the liver for a longer time than did a free drug [33]. One related point should be noted: it is evident that the biologically inert property of the PEG outer shell works efficiently to evade the MPS's very rapid micelle uptake, and, consequently, supports the micelle's long-circulation behavior in the bloodstream; however, this evasion was not perfect, providing a certain degree of the MPS uptake. In any case, because of this accumulation behavior of the micelle at the liver, strong liver toxicity was worrisome, but animal experiments and clinical results of various studies indicated that liver toxicities of the polymeric micelle systems were no more than those of the corresponding free drugs [9,14,15,33]. A possible reason for this mild liver toxicity is that the polymeric micelles accumulate only at liver's Kupffer cells, not at the liver's parenchymal cells (hepatocyte). As reported in our reference [9], the liver toxicities of doxorubicin-containing micelle evaluated with AST and ALT values were found to be milder than free doxorubicin. However, a further study is required for elucidation on this point.

The current study asserts that the MPS was activated in association with its uptake of the polymeric micelle, and that as a result of this activation, the MPS became foamy cells. In relation to the ABC phenomenon, an immunohistological observation was performed for IgM-expressing lymphocytes in the spleen at a high dose (200 mg/kg×5). However, no change in the number of IgM-expressing lymphocytes was observed in the spleen (data not shown). At present, the fate of the micelles that accumulated in the MPS cells has not been examined.

Interestingly, the current study found the biotinylated micelles in the blood vessels of tumors' peripheries (capsules) a very short time after the inoculation (1 h) and in the tumors' blood vessels 1 day after the injection. By using HPLC or radioisotope measurements of the accumulated amounts at tumor mass, preceding reports were able to show the tumor-selective accumulation of the polymeric micelles [2,10,16,27,34,35]. In these reports, the polymeric micelles showed the highest tumor accumulation at 24 h post intravenous injection. Thrombus seems at least in parts to be related to this micelle retention in the tumor blood vessels shown in Fig. 7. The EPR effect is known to facilitate the selective accumulation of the micelles at tumors. We observed much stronger micelle image in the blood vessel than in the tumor tissue 1 day after the injection with the immunostaning as shown in Fig. 7a. This observation suggests that the micelle-accumulation mechanism at specific sites of tumors is quicker than the accumulation driven by the EPR effect. However, only further studies can yield rigid evidence about the specific accumulation of micelles in the tumor blood vessels and the tumor tissues, because the research community generally believes that, when immunohistochemistry is the means, detection of dispersed micelles is more difficult to achieve than is detection of aggregates of micelles; and another general belief in the research community is that only dispersed micelles (not aggregated micelles) can be delivered by means of the EPR effect. (As described in the Results section, the micelles were found in tumor vasculatures in a highly concentrated manner, implying that the observed micelles were aggregates of the micelles rather than dispersed micelles.)

5. Conclusion

In this study's detailed histological examination, no pathological abnormality was observed for a systemic injection of PEG-P(Asp(Bzl)) polymeric micelles. The only marked change was activation of the MPS. These results confirmed the high safety of polymeric micelle drug carriers, but suggested the need of further investigation into polymeric micelles' interactions with the MPS. The immunohistochemical analyses also revealed very rapid and specific accumulation of the micelle in the vasculatures of tumor capsule of rat ascites hepatoma AH109A.

Acknowledgments

This work was supported by Grants-in-Aids from the Ministry of Health, Labour and Welfare of Japan. M. Nishihara, T. Yamamoto and M. Yokoyama acknowledge support from the Program for Promoting the Establishment of Strategic Research Centers, Special Coordination Funds for Promoting Science and Technology, and the Ministry of Education, Culture, Sports, Science, and Technology, Japan.

Please cite this article as: T. Kawaguchi et al., Histological study on side effects and tumor targeting of a block copolymer micelle on rats, J. Control. Release (2009), doi:10.1016/j.jconrel.2009.02.011

References

[1] M. Yokoyama, M. Miyauchi, N. Yamada, T. Okano, Y. Sakurai, K. Kataoka, S. Inoue, Characterization and anticancer activity of the micelle-forming polymeric anticancer drug adriamycin-conjugated poly(ethylene glycol)-poly(aspartic acid) block copolymer, Cancer Res. 50 (1990) 1693–1700.

[2] M. Yokoyama, T. Okano, Y. Sakurai, S. Fukushima, K. Okamoto, K. Kataoka, Selective delivery of adriamycin to a solid tumor using a polymeric micelle carrier system, J. Drug Target. 7 (1999) 171–186.

[3] R. Sevic, A. Eisenbberg, D. Maysinger, Block copolymer micelles as delivery vehicles of hydrophobic drugs: micelle–cell interactions, J. Drug Target. 14 (2006) 343–355.

[4] D. Sutton, N. Nasongkla, E. Blanco, J. Gao, Functionalized micelle systems for cancer targeted drug delivery, Pharm. Res. 24 (2007) 1029–1046.

[5] S.C. Kim, D.W. Kim, Y.H. Shim, J.S. Bang, H.S. Oh, S.W. Kim, M.H. Seo, In vivo evaluation of polymeric micellar paclitaxel formulation: toxicity and efficacy, J. Control. Release 72 (2001) 191–202.

[6] T.-Y. Kim, D.-W. Kim, J.-Y. Chung, S.G. Shin, S.C. Kim, D.S. Heo, N.K. Kim, Y.-J. Bang, Phase I and pharmacokinetic study of Genexol-PM, a cremophor-free, polymeric micelle-formulated paclitaxel, in patients with advanced malignancies, Clin. Cancer Res. 10 (2004) 3708–3716.

[7] Y. Matsumura, H. Maeda, A new concept for macromolecular therapeutics in cancer chemotherapy: mechanism of tumoritropic accumulation of proteins and the antitumor agent smancs, Cancer Res. 46 (1986) 6387–6392.

[8] H. Maeda, L.W. Seymour, Y. Miyamoto, Conjugates of anticancer agents and polymers: advantages of macromolecular therapeutics in vivo, Bioconjug. Chem. 3 (1992) 351–361.

[9] H. Uchino, Y. Matsumura, T. Negishi, F. Koizumi, T. Hayashi, T. Honda, N. Nishiyama, K. Kataoka, S. Naito, T. Kakizoe, Cisplatin-incorporated polymeric micelle (NC-6004) can reduce nephrotoxicity and neurotoxity of cisplatin in rats, Br. J. Cancer 19 (2005) 678–687.

[10] T. Hamaguchi, Y. Matsumura, M. Suzuki, K. Shimizu, R. Goda, I. Nakamura, I. Nakatomi, M. Yokoyama, K. Kataoka, T. Kakizoe, NK105, a paclitaxel-incorporating micellar nanoparticle formulation, can extend in vivo antitumor activity and reduce the neurotoxicity of paclitaxel, Br. J. Cancer 92 (2005) 1240–1246.

[11] H. Uchino, Y. Matsumura, T. Negishi, F. Koizumi, T. Hayashi, T. Honda, N. Nishiyama, K. Kataoka, S. Naito, T. Kakizoe, Cisplatin-incorporated polymeric micelle (NC-6004) can reduce nephrotoxicity and neurotoxity of cisplatin in rats, Br. J. Cancer 19 (2005) 678–687.

[12] Y. Mizumura, Y. Matsumura, M. Yokoyama, T. Okano, T. Kawaguchi, F. Moriyasu, T. Kakizoe, Incorporation of the anticancer agent KRN5500 into polymeric micelles diminishes the pulmonary toxicity, Jpn. J. Cancer Res. 93 (2002) 1273–1243.

[13] T. Negishi, F. Koizumi, H. Uchino, J. Kuroda, T. Kawaguchi, S. Naito, Y. Matsumura, NK105, a paclitaxel-incorporating micellar nanoparticle, is a more potent radiosensitising agent compared to free paclitaxel, Br. J. Cancer 95 (2006) 601–606.

[14] Y. Matsumura, T. Hamaguchi, T. Ura, K. Muro, Y. Yamada, Y. Shimada, K. Shirao, T. Otsuka, H. Ueno, M. Ikeda, N. Watanabe, Phase I clinical trail and pharmacokinetic evaluation of NK911, a micelle-encapsulated doxorubicin, Br. J. Cancer 91 (2004) 1775–1781.

[15] T. Hamaguchi, K. Kato, H. Yasui, C. Morizane, M. Ikeda, H. Ueno, K. Muro, Y. Yamada, T. Okusaka, K. Shirao, Y. Shimada, H. Nakahama, Y. Matsumura, A phase I and pharmacokinetic study of NK105, a paclitaxel-incorporating micellar nanoparticle formulation, Br. J. Cancer 97 (2007) 170–176.

[16] F. Koizumi, M. Kitagawa, T. Negishi, T. Onda, S. Matsumoto, T. Hamaguchi, Y. Matsumura, Novel SN-38-incorporating polymeric micelles, NK012, eradicate vascular endothelial growth factor-secreting bulky tumors, Cancer Res. 66 (2006) 10048–10056.

[17] M. Sumitomo, F. Koizumi, T. Asano, A. Horiguchi, K. Ito, T. Asano, T. Kakizoe, M. Hayakawa, Y. Matsumura, Novel SN-38-incorporated polymeric micelle, NK012, strongly suppresses renal cancer progression, Cancer Res. 68 (2008) 1631–1635.

[18] D.C. Drummond, D. Kirpotin, C. Benz, J.W. Park, K. Hong, Liposomal drug delivery systems for cancer therapy, in: D.M. Brown (Ed.), Drug Delivery Systems in Cancer Therapy, Humana Press Inc., Totowa, 2004, pp. 191–213.

[19] P.R. Hamann, M.S. Berger, Mylotarg: the first antibody-targeted chemotherapy agent, in: M. Page (Ed.), Tumor Targeting in Cancer Therapy, Humana Press Inc., Totowa, 2002, pp. 239–254.

[20] A.V. Kabanov, J. Zhu, Luronic block copolymers for drug and gene delivery, in: G.S. Kwon (Ed.), Plymeric Drug Delivery Systems, Taylor & Francis, Boca Raton, 2005, pp. 577–613.

[21] E.V. Batrakova, S. Li, W.F. Elmquist, D.W. Miller, V.Y. Alakhov, A.V. Kabanov, Mechanism of sensitization of MDR cancer cells by Pluronic block copolymers: selective energy depletion, Br. J. Cancer 85 (2001) 1987–1997.

[22] E.T.M. Dams, P. Laverman, W.J.G. Oyen, G. Strom, G.L. Scherphof, J.W.M. van der Meer, F.H.M. Coretens, O.C. Boerman, Accelerated blood clearance and altered biodistribution of repeated injections of sterically stabilized liposomes, J. Pharmacol. Exp. Ther. 292 (2000) 1071–1079.

[23] T. Ishida, M. Ichihara, X. Wang, K. Yamamoto, J. Kimura, E. Majima, H. Kiwada, Injection of PEGylated liposomes in rats elicits PEG-specific IgM, which is responsible for rapid elimination of a second dose of PEGylated liposomes, J. Control Release 112 (2006) 15–25.

[24] T. Ishida, H. Kiwada, Accelerated blood clearance (ABC) phenomenon upon repeated injection of PEGylated liposomes, Int. J. Pharm. 345 (2008) 56–62.

[25] H. Koide, T. Asai, K. Hatanaka, T. Urakami, T. Ishii, E. Kenjo, M. Nishihara, M. Yokoyama, T. Ishida, H. Kiwada, and N. Oku, The particle size-dependent occurrence of accelerated blood clearance phenomenon, Int. J. Pharm, in press.

[26] M. Watanabe, K. Kawano, M. Yokoyama, P. Opanasopit, T. Okano, Y. Maitani, Preparation of camptothecin-loaded polymeric micelles and evaluation of their incorporation and circulation stability, Int. J. Pharm. 308 (2006) 183–189.

[27] K. Kawano, M. Watanabe, T. Yamamoto, M. Yokoyama, P. Opanasopit, T. Okano, Y. Maitani, Enhanced antitumor effect of camptothecin loaded in long-circulating polymeric micelles, J. Control Release 112 (2006) 329–332.

[28] N. Chansri, S. Kawakami, M. Yokoyama, T. Yamamoto, P. Charoensit, M. Hashida, Anti-tumor effect of all-*Trans* retinoic acid loaded polymeric micelles in solid tumor bearing mice, Pharm. Res. 25 (2008) 428–434.

[29] M. Yokoyama, P. Opanasopit, Y. Maitani, K. Kawano, T. Okano, Polymer design and incorporation method for polymeric micelle carrier system containing water-insoluble anti-cancer agent camptothecin, J. Drug Target. 12 (2004) 373–384.

[30] T. Kawaguchi, S. Imai, S. Haga, J. Morimoto, T. Honda, in: K. Watanabe (Ed.), Cancer Metastases Research, Nova Science Publisher, 2008, pp. 147–163.

[31] S.M. Hue, L. Raine, H. Fanger, Use of avidin–biotin–peroxidase complex (ABC) in immunoperoxidase techniques: a comparison between ABC and unlabeled antibody (PAP) procedures, J. Histochem. Cytochem. 29 (1981) 577–580.

[32] F.M. Muggia, Doxorubicin-polymer conjugates: further demonstration of the concept of enhanced permeability and retention, Clin. Cancer Res. 5 (1999) 7–8.

[33] M. Yokoyama, T. Okano, Y. Sakurai, H. Ekimoto, C. Shibazaki, K. Kataoka, Toxicity and antitumor activity against solid tumors of micelle-forming polymeric anticancer drug and its extremely long circulation in blood, Cancer Res. 51 (1991) 3229–3236.

[34] G.S. Kwon, S. Suwa, M. Yokoyama, T. Okano, Y. Sakurai, K. Kataoka, Enhanced tumor accumulation and prolonged circulation times of micelle-forming poly(ethylene oxide–aspartate) block copolymer–adriamycin conjugates, J. Control Release 29 (1994) 17–23.

[35] N. Nishiyama, S. Okazaki, H. Cabral, M. Miyamoto, Y. Kato, Y. Sugiyama, K. Nishio, Y. Matsumura, K. Kataoka, Novel cisplatin-incorporated polymeric micelles can eradicate solid tumors in mice, Cancer Res. 63 (2003) 8977–8983.

Please cite this article as: T. Kawaguchi et al., Histological study on side effects and tumor targeting of a block copolymer micelle on rats, J. Control. Release (2009), doi:10.1016/j.jconrel.2009.02.011

G Model
IJP-10517; No. of Pages 7

International Journal of Pharmaceutics xxx (2009) xxx–xxx

Contents lists available at ScienceDirect

International Journal of Pharmaceutics

journal homepage: www.elsevier.com/locate/ijpharm

Pharmaceutical nanotechnology

Enhanced *in vivo* antitumor efficacy of fenretinide encapsulated in polymeric micelles

Tomoyuki Okuda[a], Shigeru Kawakami[a], Yuriko Higuchi[a], Taku Satoh[b], Yoshimi Oka[b], Masayuki Yokoyama[b], Fumiyoshi Yamashita[a], Mitsuru Hashida[a,c,*]

[a] Department of Drug Delivery Research, Graduate School of Pharmaceutical Sciences, Kyoto University, Sakyo-ku, Kyoto 606-8501, Japan
[b] Kanagawa Academy of Science and Technology, KSP East 404, Sakado 3-2-1, Takatsu-ku, Kawasaki-shi, Kanagawa 213-0012, Japan
[c] Institute of Integrated Cell-Material Sciences (iCeMS), Kyoto University, Yoshida, Sakyo-ku, Kyoto 606-8501, Japan

ARTICLE INFO

Article history:
Received 3 October 2008
Received in revised form 21 January 2009
Accepted 23 January 2009
Available online xxx

Keywords:
Fenretinide
4-HPR
Retinoid
Polymeric micelle
Controlled release
Drug delivery system

ABSTRACT

Fenretinide (N-(4-hydroxyphenyl)retinamide, 4-HPR) is a synthetic retinoid with high antitumor activity against a variety of malignant cells *in vitro*, and is a promising candidate for cancer chemoprevention and chemotherapy. To enhance the antitumor efficacy of 4-HPR *in vivo*, 4-HPR were encapsulated into polymeric micelles for tumor targeting by enhanced permeability and retention effects. 4-HPR encapsulated in poly(ethylene glycol)–poly(benzyl aspartate) block copolymer micelles were prepared by the evaporation method. The mean particle size of 4-HPR encapsulated in polymeric micelles was about 173 nm. After intravenous injection into tumor-bearing mice, the delivery of 4-HPR by polymeric micelles increased the blood concentration and enhanced the tumor accumulation of 4-HPR over the injection of the 4-HPR encapsulated in oil-in-water (O/W) emulsions. Tumor growth was significantly delayed following treatment by 4-HPR encapsulated in polymeric micelles, which demonstrated the improved *in vivo* antitumor efficacy of 4-HPR. In addition, 4-HPR encapsulated in polymeric micelles did not cause any body weight loss. These results suggest that polymeric micelles are a promising and effective carrier of 4-HPR in order to enhance tumor delivery and have potential application in the treatment of solid tumor.

1. Introduction

Retinoids are a class of natural or synthetic derivatives of vitamin A that exert various biological actions on cellular growth and differentiation (Means and Gudas, 1995; Kagechika and Shudo, 2005). As a result of their unique characteristics, their application in novel cancer therapy has been progressing (Altucci and Gronemeyer, 2001; Clarke et al., 2004). In particular, fenretinide (N-(4-hydroxyphenyl)retinamide, 4-HPR), which was synthesized from all-trans retinoic acid (ATRA), is a promising candidate for cancer chemoprevention and chemotherapy, since it has higher antitumor activity and lower toxicity than other retinoids (Moon et al., 1979; Miller, 1998). It was reported that the antitumor activity of 4-HPR was through two main mechanisms: retinoic acid receptor-dependent cascade and retinoic acid receptor-independent cascade, including reactive oxygen species generation, ceramide synthesis, and proapoptotic bcl-2 family protein (Bax and Bak) induction (Hail et al., 2006; Corazzari et al., 2005). Clinical trials of 4-HPR have been progressing against breast cancer, prostate cancer, and neuroblastoma (Altucci and Gronemeyer, 2001; Clarke et al., 2004).

To date, 4-HPR has been clinically administrated using an oral gelatin capsule containing 4-HPR in corn oil and polysorbate 80 [available through the National Cancer Institute]; however, this formulation has poor bioavailability, since 4-HPR itself is too hydrophobic to pass through intestinal membrane easily (Kokate et al., 2007), and requires excessive or multiple administrations to achieve a higher blood concentration of 4-HPR (Villablanca et al., 2006). In addition, several animal studies have demonstrated that intravenously injected 4-HPR is rapidly eliminated from the body (Swanson et al., 1980; Hultin et al., 1986); therefore, the development of a targeted carrier of 4-HPR is needed to exert *in vivo* antitumor efficacy.

Polymeric micelles are a class of micelles that are formed from block copolymers typically consisting of hydrophilic and hydrophobic polymer chains (Kataoka et al., 2001; Torchilin, 2004). They are of particular interest because of their efficacy in entrapping a satisfactory amount of hydrophobic drugs within the inner core, their stability in the circulation and their ability to gradually release the drugs (Kwon, 2003). In addition, the highly hydrated outer

* Corresponding author at: Department of Drug Delivery Research, Graduate School of Pharmaceutical Sciences, Kyoto University, Sakyo-ku, Kyoto 606-8501, Japan. Tel.: +81 75 753 4525; fax: +81 75 753 4575.
E-mail address: hashidam@pharm.kyoto-u.ac.jp (M. Hashida).

0378-5173/$ – see front matter © 2009 Published by Elsevier B.V.
doi:10.1016/j.ijpharm.2009.01.019

shells of the micelles prevent reticuloendothelial system (RES) uptake and inhibit intermicellar aggregation of their hydrophobic inner cores. The characteristics of these polymeric micelles could be an advantage for passive delivery and to extravasate the drug at tumor sites by enhanced permeability and retention (EPR) effects (Maeda, 2001). In our previous report, we demonstrated that poly(ethylene glycol)–poly(aspartate) block copolymer micelles modified with benzyl groups could stably encapsulate 4-HPR and enhanced blood retention of 4-HPR after intravenous injection into mice (Okuda et al., 2008). This observation prompted us to investigate the potential use of polymeric micelles to enhance tumor retention and *in vivo* antitumor efficacy of 4-HPR in tumor-bearing mice.

In this study, we extended our previous study and tumor distribution and antitumor efficacy of 4-HPR encapsulated in poly(ethylene glycol)–poly(aspartate) block copolymer micelles modified with benzyl groups after intravenous injection were examined in mice bearing murine melanoma B16BL6 tumors. As a control pharmaceutical formulation of 4-HPR, oil-in-water (O/W) or PEGylated O/W emulsions were selected because of their preparation characteristics for delivery of highly lipophilic drugs (Tamilvanan, 2004).

2. Materials and methods

2.1. Materials

4-HPR was purchased from Tokyo Chemical Industry, Co. Ltd. (Tokyo, Japan). Egg yolk phosphatidylcholine (EggPC) and 3-(4,5-dimethyl-2-thiazoyl)-2,5-diphenyl-2H tetrazolium bromide (MTT) were purchased from Sigma–Aldrich (St. Louis, MO, USA). Soybean oil (SO) and ATRA were purchased from Wako Pure Chemicals Industry, Ltd. (Osaka, Japan). Acetonitrile (HPLC grade) and acetic acid (HPLC grade) were purchased from Nacalai Tesque, Inc. (Kyoto, Japan). Distearoylphosphatidylethanolamine-N-[methoxy(polyethylene glycol)-2000] (PEG-DSPE) was purchased from Nippon Oil and Fats Co. (Tokyo, Japan). Fetal bovine serum (FBS) was obtained from Biowhittaker (Walkersville, MD). Dulbecco's modified Eagle's medium (DMEM), phosphate-buffered saline (PBS), and Hank's balanced saline solution (HBSS) were purchased from Nissui Pharmaceutical Co., Ltd. (Tokyo, Japan). All other chemicals were of the highest purity available.

2.2. Synthesis of block copolymer

Poly(ethylene glycol)–poly(aspartic acid) (PEG–P(Asp)) block copolymer was obtained by alkaline hydrolysis of poly(ethylene glycol)–poly(β-benzyl-L-aspartate) (PEG–PBLA), as reported previously (Opanasopit et al., 2004). Briefly, the molecular weight of poly(ethylene glycol) (PEG) chain was 5000 and the average number of aspartic acid units was 27. Approximately 75% of the aspartic acid residues in poly(aspartic acid) chain were converted to the β-amide form by alkaline hydrolysis during the synthesis of this block copolymer. A hydrophobic benzyl group was bound to 77% of the poly(aspartic acid) residues by an ester-forming reaction between benzyl bromide and PEG–P(Asp), as reported previously (Yokoyama et al., 2004). Briefly, PEG–P(Asp) block copolymer was dissolved in N,N-dimethylformamide (DMF) and added to benzyl bromide along with a catalyst, 1,8-diazabicyclo[5,4,0]7-undecene (DBU). The reaction mixture was stirred at 50 °C for 15.5 h. Polymer was obtained by precipitation in excess of diethyl ether and collected by filtration. The dried polymer was dissolved in dimethyl sulfoxide (DMSO), and then 6N HCl was added, followed by dialysis against distilled water and finally, freeze-drying.

For determination of the polymer composition, such as the number of aspartic acid units and the benzyl ester content, ^{1}H NMR measurements were carried out on a 1% solution in 6D-DMSO containing 3% trifluoroacetic acid using a Varian Unity Inova NMR spectrometer at 400 MHz.

2.3. Preparation of 4-HPR encapsulated in polymeric micelles

4-HPR encapsulated in polymeric micelles was prepared by a conventional evaporation method (Kawakami et al., 2005; Chansri et al., 2008). Briefly, 4-HPR and polymer were dissolved in chloroform. After vacuum drying and desiccation, PBS (pH 7.4) was added for suspension in a bath sonicator for 3 min. The suspension was sonicated for 3 min (200 W) at 75 °C using a probe sonicator (US 300, Nissei, Inc., Tokyo, Japan). The preparation was centrifuged at 1400 × *g* for 10 min before the supernatant was passed through a 0.45 μm filter.

2.4. Preparation of 4-HPR encapsulated in O/W emulsions and PEGylated O/W emulsions

4-HPR encapsulated in O/W emulsions was prepared based on our previous reports (Takino et al., 1994; Chansri et al., 2006). Briefly, 4-HPR, EggPC, and SO (30:150:150, weight ratio) were dissolved in chloroform. After vacuum drying and desiccation, PBS (pH 7.4) was added for suspension in a bath sonicator for 3 min. The suspension was sonicated for 30 min (200 W) at 4 °C using a probe sonicator (US 300, Nissei, Inc., Tokyo, Japan). 4-HPR encapsulated in PEGylated O/W emulsions, composed of 4-HPR, EggPC, PEG-DSPE, and SO (30:105:45:150, weight ratio), was also prepared using this protocol.

2.5. Characterization of the formulations

The concentration of 4-HPR in the preparations was determined by UV absorption at 370 nm (UV–vis Spectrophotometer, Shimazu Co. Ltd., Kyoto, Japan) after dissolving in DMSO (the preparations: DMSO = 10:990, volume ratio). The recovery of 4-HPR was calculated from the concentration of 4-HPR in the preparations (C_P) as follows:

$$\text{Recovery}(\%) = \frac{C_P(\text{mg/mL}) \times \text{added PBS(mL)}}{\text{initial amount of 4-HPR(mg)}} \times 100$$

On the other hand, the recovery of polymer was defined as 100% because of high solubility of polymer in PBS (>50 g/L). The particle sizes and polydispersion indexes of the preparations were measured by Zetasizer Nano Series (Malvern Instruments Ltd., Worcestershire, UK).

2.6. Animals

Male C57BL/6 mice (4 weeks old, 14–19 g) were purchased from the Shizuoka Agricultural Cooperative Association for Laboratory Animals (Shizuoka, Japan). Animals were maintained under conventional housing conditions. All animal experiments were carried out in accordance with the guidelines for Animal Experiments of Kyoto University.

2.7. Tumor cells

Murine melanoma B16BL6 cells were obtained from the Cancer Chemotherapy Center of the Japanese Foundation for Cancer Research (Tokyo, Japan). They were grown in DMEM supplemented with 10% heat-inactivated FBS, 0.15% $NaHCO_3$, 100 units/mL penicillin, and 100 μg/mL streptomycin at 37 °C in humidified air containing 5% CO_2.

Please cite this article in press as: Okuda, T., et al., Enhanced *in vivo* antitumor efficacy of fenretinide encapsulated in polymeric micelles. Int J Pharm (2009), doi:10.1016/j.ijpharm.2009.01.019

2.8. MTT assay

MTT assay was performed by the method described previously (Kawakami et al., 2006). B16BL6 cells were placed on a 96-well cluster dish at a density of 3×10^3 cells/0.28 cm^2. Twenty-four hours later, medium containing various concentrations of 4-HPR, empty polymeric micelles, and 4-HPR encapsulated in polymeric micelles was added to the plates. At each exposure time point, the medium was removed and 5 mg/mL MTT solution was added to each well. Cells were incubated for 4 h at 37 °C in 5% CO_2 and then 10% sodium dodecyl sulfate (SDS) solution was added, followed by incubation overnight to dissolve formazan crystals. An absorbance was measured at wavelengths of 570 nm in a microplate photometer (Bio-Rad Model 550, Bio-Rad Laboratories, Inc., Hercules, CA, USA). IC_{50} values were determined from dose-response curves by a nonlinear regression analysis using MULTI program developed by Yamaoka et al. (Yamaoka et al., 1981) and represent the concentration required to inhibit cell viability by 50%.

2.9. Tumor-bearing mouse model

After harvesting by trypsin, B16BL6 cells were prepared at a concentration of 4×10^6 cells/mL by HBSS. Then, 0.05 mL of the cell suspension (2×10^5 cells) was inoculated subcutaneously in the lower back of each C57BL/6 mouse. A solid tumor was observed within 7 days after tumor inoculation.

2.10. In vivo distribution study

4-HPR encapsulated in polymeric micelles, O/W emulsions, and PEGylated O/W emulsions were adjusted to 7.5 mg/mL as 4-HPR. On 14 days after tumor inoculation, they were intravenously injected into the tail vein of B16BL6-bearing mice at a dose of 75 mg/kg as 4-HPR. At each collection time point, blood was collected from the vena cava under anesthesia, and mice were killed for tumor excision. Blood was centrifuged at 5000 × *g* for 5 min at 4 °C before 200 μL of plasma was collected. The plasma was added to 400 μL of acetonitrile and 4 μL of 2 mg/mL ATRA (dissolved in ethanol) as an internal standard and vortexed. Part 0.2 g of the excised tumor was collected and added to 500 μL of acetonitrile and 5 μL of 2 mg/mL ATRA, followed by sonication using a bath sonicator for 15 min. The extract from plasma and tumor was centrifuged at 13,000 × *g* for 3 min at 4 °C, and the supernatant was collected and passed through a 0.45 μm filter. The filtrated extract was analyzed by HPLC.

2.11. HPLC conditions

The extract was analyzed with a high-performance liquid chromatograph device, consisting of a system controller (SLC-10A VP, Shimazu Co. Ltd., Kyoto, Japan), a UV–vis detector (SPD-10A VP, Shimazu Co. Ltd., Kyoto, Japan), an auto injector (SIL-10A, Shimazu Co. Ltd., Kyoto, Japan), and a HPLC pump (LC-10AS, Shimazu Co. Ltd., Kyoto, Japan). The UV–vis detector was set at 350 nm. A C18 reverse-phase column (ODS-A 150 mm × 4.6 mm, YMC Co. Ltd., Kyoto, Japan) was used. The mobile phase consisted of acetonitrile:water:acetic acid (80:19:1, volume ratio) delivered at a flow rate of 1 mL/min. The injection volume was 50 μL. All samples were analyzed at room temperature.

2.12. Pharmacokinetic analysis

Pharmacokinetic parameters including the half-life ($t_{1/2}$), the area under the concentration versus time curve ($AUC_{t-\infty}$), the total body clearance (CL_{tot}), the volume of distribution at steady state (V_{dss}), and the mean residence time (MRT) were all calculated by moment analysis program developed by Yamaoka et al. (1978).

2.13. In vivo antitumor efficacy in tumor-bearing mice

On 8 days after tumor inoculation when the tumor volume reached approximately 100 mm^3, each treatment was started. 4-HPR encapsulated in polymeric micelles and O/W emulsions was intravenously injected into the tail vein of B16BL6-bearing mice at a dose of 75 mg/(kg day) as 4-HPR. The dose of empty polymeric micelles was 375 mg/(kg day) as polymer, which was an equivalent does to 4-HPR encapsulated in polymeric micelles. In the control groups, PBS was administrated. Each treatment was performed at 10 mL/(kg day) on 8, 10, and 12 days after tumor inoculation. Tumor diameter and body weight were measured for each mouse at 2-day intervals after the treatment started. Tumor volume was calculated as follows:

$$\text{Tumor volume} = \frac{\pi}{6} \times LW^2$$

where L is the long diameter and W is the short diameter.

2.14. Statistical analysis

Statistical comparison was performed by Student's *t*-test for two groups, and Dunnett's test for multiple groups. $P < 0.05$ was considered significant.

3. Results

3.1. Characteristics of 4-HPR encapsulated in polymeric micelles

Poly(ethylene glycol)–poly(benzyl aspartate) block copolymer was successfully synthesized from PEG–P(Asp), and about 77% of the aspartic residues were esterified with benzyl groups as reported previously (Opanasopit et al., 2004). The recovery of 4-HPR achieved approximately 70% in polymer/4-HPR weight ratio at 2.5 and 3.0 (Fig. 1). Therefore, polymer/4-HPR weight ratio was fixed at 2.5 in the following experiments. The mean particle size of polymeric micelles was about 173 nm (Fig. 2). On the other hand, the mean particle sizes of O/W emulsions and PEGylated O/W emulsions were about 176 and 178 nm, respectively, similar to polymeric micelles. The polydispersion indexes of polymeric micelles, O/W

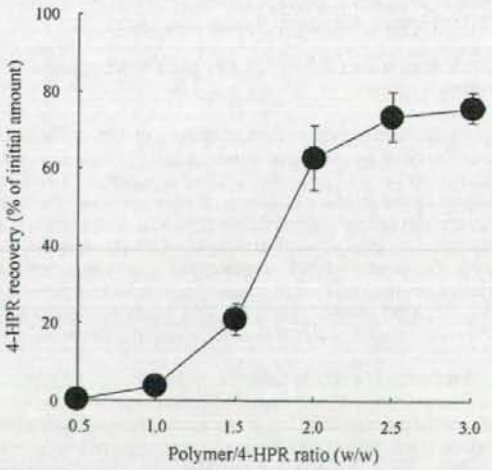

Fig. 1. Effect of polymer/4-HPR weight ratio on encapsulation of 4-HPR into prepared polymeric micelles. 4-HPR encapsulated in polymeric micelles was prepared at various weight ratio for 1 mg 4-HPR, and 4-HPR recovery was calculated. Each value represents the mean ± S.D. ($n = 4$).

Please cite this article in press as: Okuda, T., et al., Enhanced *in vivo* antitumor efficacy of fenretinide encapsulated in polymeric micelles. Int J Pharm (2009), doi:10.1016/j.ijpharm.2009.01.019

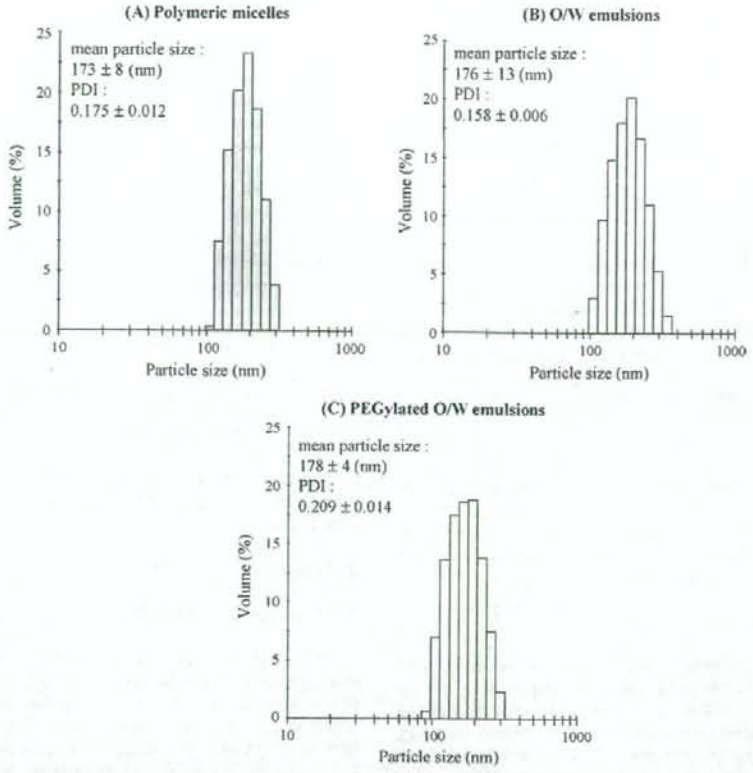

Fig. 2. Size distributions, mean particle sizes, and polydispersion indexes (PDI) of 4-HPR encapsulated in polymeric micelles (A), 4-HPR encapsulated in O/W emulsions (B), and 4-HPR encapsulated in PEGylated O/W emulsions (C). Each value of represents the mean ± S.D. ($n = 3$).

emulsions, and PEGylated O/W emulsions were about 0.175, 0.158, and 0.209, respectively, suggesting the narrow size distribution of these preparations. Furthermore, the particle size of 4-HPR encapsulated in polymeric micelles remained constant over 1 month at room temperature, 4, and −30 °C (data not shown).

3.2. *In vitro antitumor activity of 4-HPR and 4-HPR encapsulated in polymeric micelles*

For evaluating *in vitro* antitumor activity of 4-HPR and 4-HPR encapsulated in polymeric micelles against B16BL6 cells, MTT assay was performed. The *in vitro* antitumor activity of 4-HPR was enhanced as the increase of dose and exposure time (Fig. 3(A)). IC_{50} value was settled on approximately 0.60 μg/mL at more than 24 h, suggesting full antitumor activity of 4-HPR could be obtained at 24 h. IC_{50} value of 4-HPR encapsulated in polymeric micelles (52 μg/mL at 48 h) was much larger than that of free form of 4-HPR (0.60 μg/mL at 48 h) (Fig. 3(B)). This result may indicate the stable encapsulation of 4-HPR into polymeric micelles in medium.

3.3. *Distribution of 4-HPR in tumor-bearing mice*

The blood concentration and tumor accumulation of 4-HPR after intravenous injection of 4-HPR encapsulated in polymeric micelles were evaluated in B16BL6-bearing mice (Fig. 4) and compared with those of 4-HPR encapsulated in O/W emulsions or PEGylated O/W emulsions as control. The blood concentration of 4-HPR encapsulated in polymeric micelles was significantly higher than those of 4-HPR encapsulated in O/W emulsions and PEGylated O/W emulsions, suggesting that polymeric micelles could enhance the blood retention of 4-HPR compared with O/W emulsions and PEGylated O/W emulsions. Moreover, the tumor accumulation of 4-HPR encapsulated in polymeric micelles was significantly higher and prolonged for 48 h compared with O/W emulsions and PEGylated O/W emulsions. Pharmacokinetic parameters of 4-HPR encapsulated in polymeric micelles, O/W emulsions, and PEGylated O/W emulsions were shown in Table 1. The area under the curve ($AUC_{0-\infty}$) in blood was approximately 23.9 times higher for 4-HPR encapsulated in polymeric micelles than for that in O/W emulsions. The $t_{1/2}$ in blood was approximately 5.02 times longer for 4-HPR encapsulated in polymeric micelles than for that in O/W emulsions. Furthermore, the maximum concentration (C_{max}), and the $AUC_{0-\infty}$ in tumors were approximately 3.03 and 16.9 times higher for 4-HPR encapsulated in polymeric micelles than for that in O/W emulsions, respectively. The $t_{1/2}$ in tumors was approximately 5.63 times longer for 4-HPR encapsulated in polymeric micelles than for that in O/W emulsions.

3.4. *In vivo antitumor efficacy of 4-HPR encapsulated in polymeric micelles in tumor-bearing mice*

In vivo antitumor efficacy of 4-HPR encapsulated in polymeric micelles was evaluated in B16BL6-bearing mice after intravenous injection of PBS (control), empty polymeric micelles, 4-HPR encapsulated in O/W emulsions, and 4-HPR encapsulated in polymeric micelles. Each treatment was performed on 8, 10, and 12 days (total

Please cite this article in press as: Okuda, T., et al., Enhanced *in vivo* antitumor efficacy of fenretinide encapsulated in polymeric micelles. Int J Pharm (2009), doi:10.1016/j.ijpharm.2009.01.019

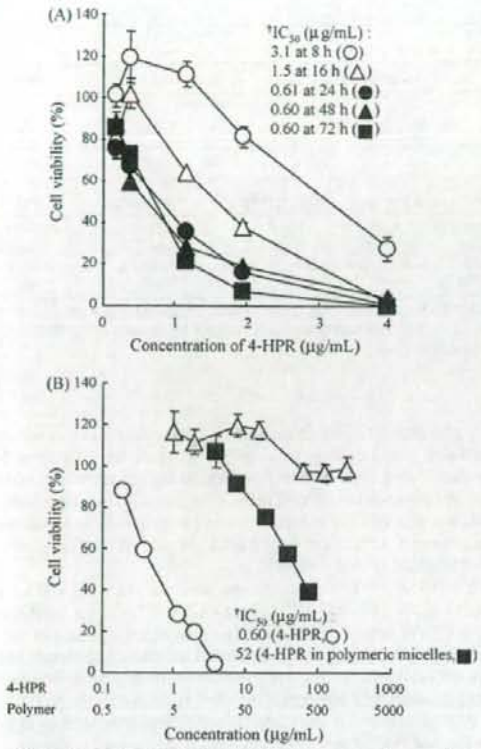

†IC_{50} values were determined from dose-response curves by a nonlinear regression analysis using MULTI program developed by Yamaoka et al. (Yamaoka et al., 1981) and represent the concentration required to inhibit cell viability by 50 %.

Fig. 3. *In vitro* antitumor activity of 4-HPR and 4-HPR encapsulated in polymeric micelles against B16BL6 cells. (A) Time and concentration dependence of *in vitro* antitumor activity of 4-HPR. Cell viability was measured by MTT method at 8 h (open circle), 16 h (open triangle), 24 h (filled circle), 48 h (filled triangle), and 72 h (filled square) after treatment. (B) *In vitro* antitumor activity of 4-HPR (open circle), empty polymeric micelles (shade triangle), and 4-HPR encapsulated in polymeric micelles (filled square) at 48 h after treatment. Each value represents the mean ± S.D. (n = 3–4).

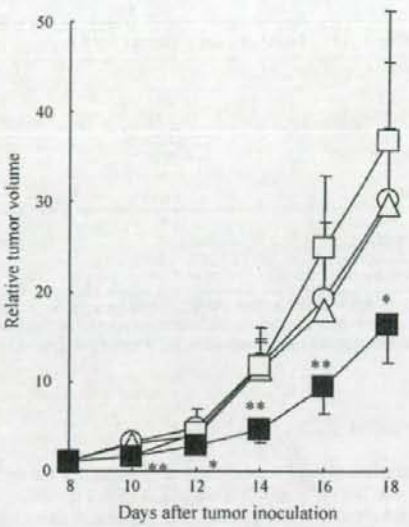

Fig. 5. Relative tumor volume of B16BL6-bearing mice after intravenous injection of PBS (open circle), empty polymeric micelles (open triangle), 4-HPR encapsulated in O/W emulsions (open square), and 4-HPR encapsulated in polymeric micelles (filled square). 4-HPR encapsulated in O/W emulsions and 4-HPR encapsulated in polymeric micelles were intravenously injected into mice at a dose of 75 mg/kg as 4-HPR on 8, 10, 12 days after tumor inoculation. The dose of empty polymeric micelles was 375 mg/kg as polymer, which was equivalent dose to 4-HPR encapsulated in polymeric micelles. Each value represents the mean ± S.D. (n = 6–12). Statistically significant differences compared with PBS-treated groups (**P < 0.01; *P < 0.05).

three times) after tumor inoculation. Only 4-HPR encapsulated in polymeric micelles significantly delayed tumor growth in B16BL6-bearing mice as compared with PBS (Fig. 5), while did not cause any significant weight loss (data not shown). On 18 days after tumor inoculation, approximately 55% of tumor growth inhibition was observed in mice treated with 4-HPR encapsulated in polymeric micelles. On the other hand, empty polymeric micelles and 4-HPR encapsulated in O/W emulsions did not have any effect on tumor growth (Fig. 5).

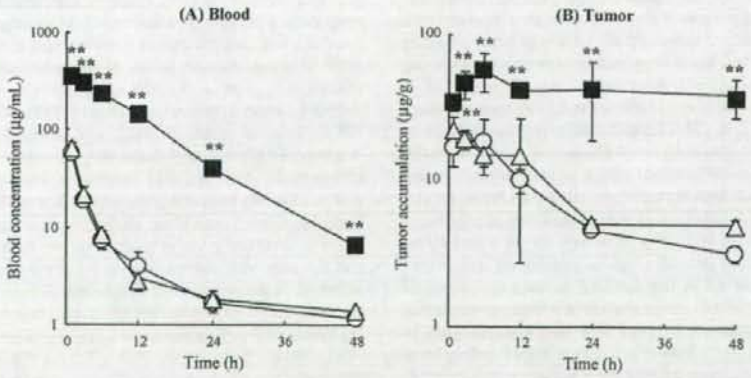

Fig. 4. Blood concentration (A) and tumor accumulation (B) of 4-HPR following intravenous injection of 4-HPR encapsulated in O/W emulsions (open circle), 4-HPR encapsulated in PEGylated O/W emulsions (open triangle), and 4-HPR encapsulated in polymeric micelles (filled square), into B16BL6-bearing mice. Each formulation was intravenously injected at 75 mg/kg dose of 4-HPR on 14 days after tumor inoculation. At indicated time point, blood and tumor were collected and amount of 4-HPR was measured by HPLC. Each value represents the mean ± S.D. (n = 3–6). Statistically significant differences compared with 4-HPR encapsulated in O/W emulsions (**P < 0.01).

Please cite this article in press as: Okuda, T., et al., Enhanced *in vivo* antitumor efficacy of fenretinide encapsulated in polymeric micelles. Int J Pharm (2009), doi:10.1016/j.ijpharm.2009.01.019

Table 1
Pharmacokinetic parameters for blood and tumor concentration of 4-HPR after intravenous injection of 4-HPR encapsulated in polymeric micelles, 4-HPR encapsulated in O/W emulsions, and 4-HPR encapsulated in PEGylated O/W emulsions into B16BL6-bearing mice.

Formulation	$t_{1/2}$ (h)	$AUC_{0-\infty}$ (μg h/mL)	CL_{tot} (mL/h kg)	V_{dss} (mL/kg)	MRT (h)
Blood[a]					
O/W emulsions	1.73	197	382	843	2.21
PEGylated O/W emulsions	1.73	225	333	737	2.21
Polymeric micelles	8.68	4717	15.9	199	12.5

Formulation	C_{max} (μg/g)	T_{max} (h)	$t_{1/2}$ (h)	$AUC_{0-\infty}$ (μg h/g)	CL_{tot} (g/h kg)	V_{dss} (g/kg)	MRT (h)
Tumor							
O/W emulsions	18.7	3	17.7	430	175	4242	14.3
PEGylated O/W emulsions	21.7	1	20.1	509	147	4038	27.4
Polymeric micelles	56.6	6	99.8	7264	10.3	1505	146

$t_{1/2}$ = half-life; AUC = area under the curve; CL_{tot} = total body clearance; V_{dss} = volume of distribution at steady state; MRT = mean residence time; C_{max} = maximum concentration; T_{max} = time of maximum concentration; parameters were calculated from the mean value of three to six mice by moment analysis developed by Yamaoka et al. (1978).
[a] Parameters in blood were calculated for the initial phase of the experiment until 6 h after intravenous injection.

4. Discussion

Nano-particulate formulation is very attractive for intravenous injection of lipophilic drugs including 4-HPR. Previously, we have developed poly(ethylene glycol)–poly(aspartate) block copolymer micelles modified with benzyl groups and demonstrated their properties of stable encapsulation and enhanced blood circulation time of 4-HPR in mice (Okuda et al., 2008). In this study, we further investigated its disposition characteristics and pharmacological effects of 4-HPR encapsulated in polymeric micelles in tumor-bearing mice. We demonstrated here for the first time that *in vivo* antitumor effect was achieved by intravenous injection of 4-HPR encapsulated in polymeric micelles.

Spaces in the blood endothelium formed by solid tumors were reported to range between 300 and 4700 nm (Yuan et al., 1995; Hashizume et al., 2000). As shown in Fig. 2, the mean particle size of prepared polymeric micelles was approximately 173 nm. Furthermore, their mean particle size did not change for more than 1 month storage, even at room temperature (data not shown). These results suggested that they might be small enough to exert long circulating potential and pass through the endothelium of solid tumors.

As shown in Fig. 3(A), exposure to 4-HPR for more than 24 h was needed to exert high antitumor activity of 4-HPR against B16BL6 cells *in vitro*. This observation of *in vitro* antitumor characteristics of 4-HPR corresponds with a previous report (Wu et al., 2005) and in the other cancer cells (Holmes et al., 2003). Since EPR effects are known to enhance and prolong tumor distribution based on the characteristic vascular structure around tumor tissues, such passive targeting of 4-HPR to tumor tissues by EPR effects is expected to be an effective strategy for exerting *in vivo* pharmacological actions. After intravenous injection of 4-HPR encapsulated in polymeric micelles, the blood concentration of 4-HPR was extended (Fig. 4(A)). Investigating whether polymeric micelles can improve *in vivo* antitumor efficacy of 4-HPR, and the therapeutic efficacy of 4-HPR encapsulated in polymeric micelles was evaluated in B16BL6-bearing mice. As shown in Fig. 4(B), the tumor concentration of 4-HPR by 4-HPR encapsulated in polymeric micelles was from 33.9 to 56.6 μg/g of 4 HPR for 48 h and could significantly inhibit tumor growth (Fig. 5). The *in vivo* antitumor efficacy might be supported by the fact that *in vitro* IC_{50} value of 4-HPR against B16BL6 cells at more than 24 h was approximately 0.60 μg/mL. *In vitro* antitumor activity of 4-HPR encapsulated in polymeric micelles was much lower than that of 4-HPR in free form (Fig. 4(B)), but intravenously injected 4-HPR encapsulated in polymeric micelles showed the enhanced antitumor efficacy *in vivo* (Fig. 5). It might be partly explained that stably encapsulated 4-HPR was much slowly released in medium but was a little enhanced releasing by interaction with various biocomponents such as serum albumin and blood cells *in vivo*. With regard to the toxicity of 4-HPR encapsulated in polymeric micelles, no significant loss of body weight was observed in treated mice, suggesting little severe toxicity (data not shown). These results lead us to believe that enhanced *in vivo* antitumor efficacy of 4-HPR could be achieved by polymeric micelles without severe side-effects.

Lipid particles are known as conventional drug carriers, and have been already used clinically (Tamilvanan, 2004; Torchilin, 2005). In particular, O/W emulsions or PEGylated O/W emulsions can dissolve highly lipophilic drugs in the inner oil phase; however, few reports are available to compare the disposition of lipophilic drugs by encapsulation into polymeric micelles with that in these emulsions. After intravenous injection of 4-HPR encapsulated in O/W emulsions and PEGylated O/W emulsions, 4-HPR were rapidly eliminated from the blood and tumor (Fig. 4). Similarly, *in vivo* antitumor efficacy by 4-HPR encapsulated in O/W emulsion was not observed (Fig. 5). In our previous study, we systematically investigated the *in vivo* disposition of drugs with diverse lipophilicity, and concluded that the required lipophilicity of drugs for stable encapsulation into O/W emulsions was found to be 10^9 based on the partition coefficient between n-octanol and water (PC_{oct}) values (Takino et al., 1994). PC_{oct} of 4-HPR is $10^{8.03}$ (Kokate et al., 2007); therefore, 4-HPR might be rapidly released from O/W emulsions and PEGylated O/W emulsions to the blood stream by the intravenous injection.

Many factors can contribute to tumorigenesis, including inherited and acquired genetic changes, chromosomal rearrangements, epigenetic phenomena and chemical carcinogenesis. Retinoids can interfere with these events on several levels, their principal known actions being the induction of differentiation and apoptosis of tumor cells, and inhibition of tumor promotion in chemically induced cancers (Means and Gudas, 1995; Kagechika and Shudo, 2005). To date, many retinoids are candidates for the treatment of cancers (Altucci and Gronemeyer, 2001; Clarke et al., 2004); however, it is difficult to achieve therapeutic effect under *in vivo* conditions because their highly lipophilic nature and teratogenicity (Collins and Mao, 1999; Soprano and Soprano, 1995). In order to overcome these problems, we developed poly(ethylene glycol)–poly(benzyl aspartate) block copolymer micelles for 4-HPR delivery. In polymeric micelle delivery, drug encapsulation characteristics can be controlled by modification of the hydrophobic segments of block copolymers (Yokoyama et al., 2004; Watanabe et al., 2006; Okuda et al., 2008). Taking these into consideration, polymeric micelles would be effective carriers for various retinoids for cancer chemotherapy in the future.

In conclusion, we have examined the biodistribution characteristics of 4-HPR encapsulated in poly(ethylene glycol)–poly(benzyl

Please cite this article in press as: Okuda, T., et al., Enhanced *in vivo* antitumor efficacy of fenretinide encapsulated in polymeric micelles. Int J Pharm (2009), doi:10.1016/j.ijpharm.2009.01.019

aspartate) block copolymer micelles after intravenous injection in tumor-bearing mice. We have demonstrated that 4-HPR encapsulated in polymeric micelles sustained blood retention of 4-HPR, passive accumulation at tumor sites, and led to superior therapeutic benefits of 4-HPR against solid tumor in tumor-bearing mice.

Acknowledgements

This work was supported in part by Grants-in-Aid for Scientific Research from the Ministry of Education, Culture, Sports, Science, and Technology of Japan, and by Health and Labour Sciences Research Grants for Research on Advanced Medical Technology from the Ministry of Health, Labour and Welfare of Japan. T. Satoh, Y. Oka, and M. Yokoyama acknowledge support by the Program for Promoting the Establishment of Strategic Research Centers, Special Coordination Funds for Promoting Science and Technology, The Ministry of Education, Culture, Sports, Science, and Technology, Japan.

References

Altucci, L., Gronemeyer, H., 2001. The promise of retinoids to fight against cancer. Nat. Rev. Cancer 1, 181–193.
Chansri, N., Kawakami, S., Yamashita, F., Hashida, M., 2006. Inhibition of liver metastasis by all-trans retinoic acid incorporated into O/W emulsions in mice. Int. J. Pharm. 321, 42–49.
Chansri, N., Kawakami, S., Yokoyama, M., Yamamoto, T., Charoensit, P., Hashida, M., 2008. Anti-tumor effect of all-trans retinoic acid loaded polymeric micelles in solid tumor bearing mice. Pharm. Res. 25, 428–434.
Clarke, N., Germain, P., Altucci, L., Gronemeyer, H., 2004. Retinoids: potential in cancer prevention and therapy. Expert Rev. Mol. Med. 6, 1–23.
Collins, M.D., Mao, G.E., 1999. Teratology of retinoids. Annu. Rev. Pharmacol. Toxicol. 39, 399–430.
Corazzari, M., Lovat, P.E., Oliverio, S., Di Sano, F., Donnorso, R.P., Redfern, C.P., Piacentini, M., 2005. Fenretinide: a p53-independent way to kill cancer cells. Biochem. Biophys. Res. Commun. 331, 810–815.
Hail Jr., N., Kim, H.J., Lotan, R., 2006. Mechanisms of fenretinide-induced apoptosis. Apoptosis 11, 1677–1694.
Hashizume, H., Baluk, P., Morikawa, S., McLean, J.W., Thurston, G., Roberge, S., Jain, R.K., McDonald, D.M., 2000. Openings between defective endothelial cells explain tumor vessel leakiness. Am. J. Pathol. 156, 1363–1380.
Holmes, W.F., Soprano, D.R., Soprano, K.J., 2003. Comparison of the mechanism of induction of apoptosis in ovarian carcinoma cells by the conformationally restricted synthetic retinoids CD437 and 4-HPR. J. Cell. Biochem. 89, 262–278.
Hultin, T.A., May, C.M., Moon, R.C., 1986. N-(4-hydroxyphenyl)-all-trans-retinamide pharmacokinetics in female rats and mice. Drug Metab. Dispos. 14, 714–717.
Kagechika, H., Shudo, K., 2005. Synthetic retinoids: recent developments concerning structure and clinical utility. J. Med. Chem. 48, 5875–5883.
Kataoka, K., Harada, A., Nagasaki, Y., 2001. Block copolymer micelles for drug delivery: design, characterization and biological significance. Adv. Drug Deliv. Rev. 47, 113–131.
Kawakami, S., Opanasopit, P., Yokoyama, M., Chansri, N., Yamamoto, T., Okano, T., Yamashita, F., Hashida, M., 2005. Biodistribution characteristics of all-trans retinoic acid incorporated in liposomes and polymeric micelles following intravenous administration. J. Pharm. Sci. 94, 2606–2615.
Kawakami, S., Suzuki, S., Yamashita, F., Hashida, M., 2006. Induction of apoptosis in A549 human lung cancer cells by all-trans retinoic acid incorporated in DOTAP/cholesterol liposomes. J. Control. Release 110, 514–521.
Kokate, A., Li, X., Jasti, B., 2007. Transport of a novel anti-cancer agent, fenretinide across Caco-2 monolayers. Invest. New Drugs 25, 197–203.
Kwon, G.S., 2003. Polymeric micelles for delivery of poorly water-soluble compounds. Crit. Rev. Ther. Drug Carrier Syst. 20, 357–403.
Maeda, H., 2001. The enhanced permeability and retention (EPR) effect in tumor vasculature: the key role of tumor-selective macromolecular drug targeting. Adv. Enzyme Regul. 41, 189–207.
Means, A.L., Gudas, L.J., 1995. The roles of retinoids in vertebrate development. Annu. Rev. Biochem. 64, 201–233.
Miller Jr., W.H., 1998. The emerging role of retinoids and retinoic acid metabolism blocking agents in the treatment of cancer. Cancer 83, 1471–1482.
Moon, R.C., Thompson, H.J., Becci, P.J., Grubbs, C.J., Gander, R.J., Newton, D.L., Smith, J.M., Phillips, S.L., Henderson, W.R., Mullen, L.T., Brown, C.C., Sporn, M.B., 1979. N-(4-hydroxyphenyl)retinamide, a new retinoid for prevention of breast cancer in the rat. Cancer Res. 39, 1339–1346.
Okuda, T., Kawakami, S., Yokoyama, M., Yamamoto, T., Yamashita, F., Hashida, M., 2008. Block copolymer design for stable encapsulation of N-(4-hydroxyphenyl)retinamide into polymeric micelles in mice. Int. J. Pharm. 357, 318–322.
Opanasopit, P., Yokoyama, M., Watanabe, M., Kawano, K., Maitani, Y., Okano, T., 2004. Block copolymer design for camptothecin incorporation into polymeric micelles for passive tumor targeting. Pharm. Res. 21, 2001–2008.
Soprano, D.R., Soprano, K.J., 1995. Retinoids as teratogens. Annu. Rev. Nutr. 15, 111–132.
Swanson, B.N., Zaharevitz, D.W., Sporn, M.B., 1980. Pharmacokinetics of N-(4-hydroxyphenyl)-all-trans-retinamide in rats. Drug Metab. Dispos. 8, 168–172.
Takino, T., Konishi, K., Takakura, Y., Hashida, M., 1994. Long circulating emulsion carrier systems for highly lipophilic drugs. Biol. Pharm. Bull. 17, 121–125.
Tamilvanan, S., 2004. Oil-in-water lipid emulsions: implications for parenteral and ocular delivering systems. Prog. Lipid Res. 43, 489–533.
Torchilin, V.P., 2004. Targeted polymeric micelles for delivery of poorly soluble drugs. Cell. Mol. Life Sci. 61, 2549–2559.
Torchilin, V.P., 2005. Recent advances with liposomes as pharmaceutical carriers. Nat. Rev. Drug Discov. 4, 145–160.
Villablanca, J.G., Krailo, M.D., Ames, M.M., Reid, J.M., Reaman, G.H., Reynolds, C.P., 2006. Phase I trial of oral fenretinide in children with high-risk solid tumors: a report from the Children's Oncology Group (CCG 09709). J. Clin. Oncol. 24, 3423–3430.
Watanabe, M., Kawano, K., Yokoyama, M., Opanasopit, P., Okano, T., Maitani, Y., 2006. Preparation of camptothecin-loaded polymeric micelles and evaluation of their incorporation and circulation stability. Int. J. Pharm. 308, 183–189.
Wu, X.Z., Zhang, L., Shi, B.Z., Hu, P., 2005. Inhibitory effects of N-(4-hydrophenyl) retinamide on liver cancer and malignant melanoma cells. World J. Gastroenterol. 11, 5763–5769.
Yamaoka, K., Nakagawa, T., Uno, T., 1978. Statistical moments in pharmacokinetics. J. Pharmacokinet. Biopharm. 6, 547–558.
Yamaoka, K., Tanigawara, Y., Nakagawa, T., Uno, T., 1981. A pharmacokinetic analysis program (multi) for microcomputer. J. Pharmacobiodyn. 4, 879–885.
Yokoyama, M., Opanasopit, P., Okano, T., Kawano, K., Maitani, Y., 2004. Polymer design and incorporation methods for polymeric micelle carrier system containing water-insoluble anti-cancer agent camptothecin. J. Drug Target 12, 373–384.
Yuan, F., Dellian, M., Fukumura, D., Leunig, M., Berk, D.A., Torchilin, V.P., Jain, R.K., 1995. Vascular permeability in a human tumor xenograft: molecular size dependence and cutoff size. Cancer Res. 55, 3752–3756.

Please cite this article in press as: Okuda, T., et al., Enhanced *in vivo* antitumor efficacy of fenretinide encapsulated in polymeric micelles. Int J Pharm (2009), doi:10.1016/j.ijpharm.2009.01.019

Journal of Controlled Release xxx (2009) xxx–xxx

Contents lists available at ScienceDirect

Journal of Controlled Release

journal homepage: www.elsevier.com/locate/jconrel

Encapsulation of the synthetic retinoids Am80 and LE540 into polymeric micelles and the retinoids' release control

Taku Satoh [a], Yuriko Higuchi [b], Shigeru Kawakami [b], Mitsuru Hashida [b], Hiroyuki Kagechika [c], Koichi Shudo [d], Masayuki Yokoyama [a,*]

[a] Yokoyama Project, Kanagawa Academy of Science and Technology, KSP East 404, Sakado 3-2-1, Takatsu-ku, Kawasaki, Kanagawa 213-0012, Japan
[b] Department of Drug Delivery Research, Graduate School of Pharmaceutical Sciences, Kyoto University, Sakyo-ku, Kyoto 606-8501, Japan
[c] School of Biomedical Science, Tokyo Medical and Dental University, Kanda-surugadai 2-3-10, Chiyoda-ku, Tokyo 101-0062, Japan
[d] Research Foundation Itsuu Laboratory, Tamagawa 2-28-10, Setagaya-ku, Tokyo 158-0094, Japan

ARTICLE INFO

Article history:
Received 25 December 2008
Accepted 27 February 2009
Available online xxxx

Keywords:
Polymeric micelle
Retinoid
Ion-pairing
Sustained release
Controlled release

ABSTRACT

The objective of this study was to encapsulate two synthetic retinoids Am80 and LE540 into polymeric micelles and to control the retinoids' release rate in vitro. Highly efficient encapsulation yields of these retinoids were obtained for micelles forming from PEG-poly(benzyl aspartate) block copolymers in the wide range of the benzyl substitution degree. The in vitro release examination for LE540 indicated very stable encapsulation of this retinoid owing to its strongly hydrophobic nature. On the other hand, Am80 exhibited a rapid release in Dulbecco's phosphate buffer saline. An addition of a hydrophobic alkyl amine in the Am80-encapsulation process successfully led to significant retardation of the Am80 release rate. A mechanism of the retardation was considered an increase of Am80 hydrophobicity due to an ion-pairing with the alkyl amine. This paper is the first report on release control in the polymeric micelle carrier system through the ion-pairing between an encapsulated drug and an additive.

1. Introduction

Polymeric micelles are self-assembling nanostructures that are typically composed of amphiphilic block copolymers [1]. Micelles have recently received much attention as a promising drug delivery carrier because a large quantity of hydrophobic drugs can be encapsulated into the micelle core in a stable manner. In systemic administration the drug-encapsulating micelles are expected to demonstrate various advantages; e.g., long-circulation in the blood stream owing to the nano-size and the hydrated-surface property of the micelles, and selective accumulation at tumor tissues owing to the EPR effect [2].

For drug targeting with the polymeric micelle carriers, research and development have focused on hydrophobic and cytotoxic anti-cancer drugs such as doxorubicin [3], paclitaxel [4], and camptothecin and its analogues [5,6]. These drugs cause cell mortality by means of strong cellular dysfunction. We would like to explore an application of polymeric micelle delivery using another type of drug that expresses pharmacological activities by regulating cellular functions. We have selected retinoids for this purpose [7,8].

Retinoids were originally defined as vitamin A and its analogues [9]. Compounds in this family modulate specific nuclear receptors called retinoic acid and retinoid X receptors (RARs and RXRs). Each of these receptors includes three subtypes (α, β, and γ). By binding to these receptors retinoids regulate cellular events including differentiation, proliferation, and apoptosis [10,11]. All-trans retinoic acid (ATRA) is clinically approved against acute promyelocytic leukemia (APL). This is the first approval of the differentiation therapy against cancer, indicating retinoids' high potency in clinical applications [12]. In an updated definition, retinoids are expanded to include molecules that bind to RARs and RXRs [13,14], regardless of their similarity in molecular structure to vitamin A. Researchers have reported that synthetic retinoids, such as 6-[3-(1-adamantyl)-4-hydroxyphenyl]-2-naphthalene carboxylic acid (CD437) [15] and *N*-(4-hydroxyphenyl) retinamide (4-HPR) [16], have induced apoptosis in neoplasma. Although researchers have not yet fully elucidated the mechanism underlying the related actions of these synthetic retinoids, CD437- and 4-HPR-induced apoptosis includes an RAR-independent pathway. Many other synthetic retinoids have been designed to improve pharmacological effects and to decrease adverse effects [17,18].

For the current research project, we selected two synthetic retinoids, Am80 and LE540, as encapsulated drugs (Chart 1). One reason for our decision to select these retinoids is their attractive pharmacological activities. Am80, an RAR-α/β specific agonist, was approved in Japan in 2005 for relapsed or refractory APL [19]. Its antimyeloma [20] and atherosclerosis inhibition effects in vivo have also been reported [21]. Since this synthetic retinoid has little binding affinity to cellular retinoic acid-binding proteins (CRABP),

* Corresponding author.
E-mail address: yp-yokoyama2093ryo@newkast.or.jp (M. Yokoyama).

0168-3659/$ – see front matter © 2009 Published by Elsevier B.V.
doi:10.1016/j.jconrel.2009.02.024